JOURNAL OF CHEMICAL & ENGINEERING DATA

Article

pubs.acs.org/jced

An Experimental Investigation of the Solubility of CO_2 in (*N*,*N*-Dimethylmethanamide + Water)

Michael Jödecke, Álvaro Pérez-Salado Kamps, and Gerd Maurer*

Department of Mechanical and Process Engineering, University of Kaiserslautern, P.O. Box 30 49 D-67653, Kaiserslautern, Germany

ABSTRACT: New experimental results are presented for the solubility of carbon dioxide in pure liquid *N*,*N*-dimethylmethanamide {= *N*,*N*-dimethylformamide, $(CH_3)_2NC(H)O$, DMF} and in solvent mixtures of (water + DMF) at gas-free solvent mixture DMF mole fractions of about (0.05, 0.1, 0.25, 0.5, 0.75, and 0.9), temperatures of (314, 354, and 395) K, and total pressures up to about 10 MPa. Numerical values are reported for the (molality scale based) Henry's constant of CO_2 in DMF and in (water + DMF) liquid mixtures resulting from the new experimental data by applying a common extrapolation procedure. The experimental work is to provide a database for developing and testing thermodynamic models to describe the gas solubility in salt-free and salt-containing mixed aqueous solvents, as well as to test screening methods based, for example, on molecular simulation.

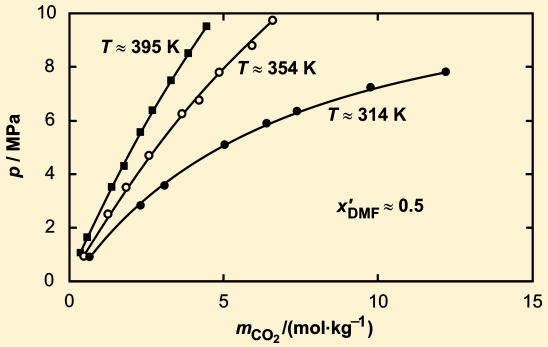

INTRODUCTION

Accurate experimental data for the solubility of gases in pure solvents and solvents mixtures are required for many applications in the chemical, pharmaceutical, and oil-related industries as well as for the development of correlations and prediction methods in molecular thermodynamics. The present publication extends previous reports of the principal investigator's group on experimental and modeling work on the physical as well as on the chemical solubility of single gases and binary gas mixtures in pure solvents as well as in solvent mixtures that have been measured over a period of nearly 25 years.[1−66]

The present work deals with the physical solubility of a single gas in binary solutions of water and an organic solvent. Hereby, the whole range of solvent compositions—from pure water to the pure organic solvent—is covered.

In the first part, new experimental results are reported for the solubility of carbon dioxide in pure *N*,*N*-dimethylmethanamide (also known as *N*,*N*-dimethylformamide and commonly abbreviated by DMF) as well as in six aqueous mixtures of DMF (mole fraction of DMF = 0.05, 0.1, 0.25, 0.5, 0.75, and 0.9) at three temperatures (314 K, 354 K, and 395 K) at pressures up to 10 MPa. The experimental results are used to determine Henry's constant for the solubility of carbon dioxide in those solvents. In the second part, the new experimental gas solubility data are correlated, applying a thermodynamic model that allows for an accurate description of gas solubility in binary mixed solvent systems covering all solvent compositions.[67] So far, this model has been successfully tested to describe the solubility of carbon dioxide in aqueous solutions of methanol,[35,67] acetone,[49,87] or the ionic liquid 1-*n*-butyl-3-methylimidazolium methylsulfate ($[bmim][CH_3SO_4]$)[66] and to describe the solubility of ammonia in aqueous solutions of methanol.[50,51] Furthermore, the influence of a single strong electrolyte (NaCl and Na_2SO_4) on the solubility of CO_2 in aqueous solutions of methanol[39,40,67−69] as well as on the solubility of NH_3 in aqueous solutions of methanol[55] has been favorably described by that model. To enable easier access to the present work the descriptions of the experimental procedures and data evaluation as well as on the correlation procedures from previous publications on related topics[48−51] are adapted and extended.

APPARATUS AND MEASURING TECHNIQUE

Details of the equipment used to measure the solubility of a gas in a given solvent as well as on the experimental procedure applied have been reported before.[6,35,48,70] Therefore, only a few characteristics are summarized here. The procedure of the experimental arrangement follows the *synthetic technique for gas solubility measurements*,[71] that is, in an experiment the pressure is determined which is required to dissolve at a constant and preset temperature an accurately known amount of a gas in an also accurately known amount of a solvent. The center of the arrangement is a thermostatted cylindrical high-pressure view cell (material = stainless steel; volume = about 30 cm^3) with sapphire windows on both ends. The amount of CO_2 charged to the cell is determined volumetrically (gravimetrically) when that amount is below (above) about 1.3 g. The amount of solvent is always determined volumetrically. When the amount of CO_2 is determined volumetrically, the gas is always charged first; that is, it is filled into the previously evacuated cell, and the amount of CO_2 is calculated (applying an appropriate equation of state[72]) from the volume of the cell and readings of temperature and pressure in the loaded cell. The volume of the

Received: December 22, 2011
Accepted: February 23, 2012
Published: March 28, 2012

cell was accurately determined at a fixed temperature by means of a high precision displacement pump (Ruska Instrument Corporation, Houston, TX, type 2241). Corrections are applied to account for the small thermal expansion when measurements are taken at other temperatures. At any temperature, the volume of the cell is known to within ± 0.1 %. The temperature is determined by calibrated platinum resistance thermometers with an uncertainty of less than 0.1 K. The pressure is determined with two calibrated pressure transducers suitable for pressures ranging up to (0.6 and 2.5) MPa, with an uncertainty of less than 0.1 % of the full scale reading. The volumetric filling was applied when the amount of CO_2 that was charged to the cell was between about (0.2 and 1.3) g. The corresponding relative uncertainty for the amount of CO_2 is about 0.3 %. There were two different procedures for charging the cell gravimetrically with CO_2. When the amount of CO_2 was below about 4 g, the evacuated cell was charged from a small condenser cylinder, and the amount of CO_2 was determined by weighing that condenser before and after the filling procedure on a high precision balance. When the amount of CO_2 was above about 4 g (at maximum it was about 15 g for the experiments with pure DMF at 314 K) the evacuated cell was at first partly filled with the solvent before CO_2 was charged from the condenser. In all such gravimetrical charges the absolute uncertainty of the mass of CO_2 charged to the cell is ± 0.012 g. The solvent is always charged via a calibrated high pressure spindle press. The volume change in that spindle press is determined from readings for the displacement of the piston, the diameter of the piston, and the density of the solvent: the density of the solvent was determined with a vibrating tube densimeter (Anton Paar GmbH, Graz, Austria). The relative uncertainty of the amount of solvent is about ± 0.2 %.

The amount of solvent charged to the cell was always slightly above the minimum amount required to dissolve the gas completely. When the filling was complete, the liquid mixture was stirred by a magnetic stirrer that is driven from the outside to achieve equilibration. Then the pressure in the cell was decreased in small steps by withdrawing tiny amounts of the liquid mixture from the cell back into the spindle press until the first small stable bubbles appear. The pressure then attained is the equilibrium pressure to dissolve the charged amount of the gas in the remaining amount of solvent at the particular fixed temperature. As the liquid mixture is almost incompressible, the amount of that mixture and in particular the amount of dissolved gas, which are withdrawn from the cell to decrease the pressure, are negligibly small.

The solubility pressure was measured with two electronic pressure transducers (from WIKA GmbH, Klingenberg, Germany) suitable for differential pressures up to (4 and 10) MPa, respectively, in connection with a mercury barometer (for measuring the atmospheric pressure). Before and after each series of measurements, the transducers were calibrated against a high precision pressure gauge (Desgranges & Huot, Aubervilliers, France). The maximum systematic uncertainty in the solubility pressure measurement results from the uncertainty of the pressure transducers (0.1 % of the transducer's full scale) and an additional contribution of about ± 0.01 MPa caused by a small temperature drift in the isolated tubes filled with the solvent, which connect the cell with the pressure transducers. That temperature drift contribution was determined in test runs.

Substances and Sample Pretreatment. Carbon dioxide (mole fraction ≥ 0.99995, from Messer-Griesheim GmbH, Ludwigshafen, Germany) was used without further purification. DMF (mass fraction ≥ 0.999, from Merck, GmbH, Darmstadt, Germany) was degassed under vacuum. Deionized water was degassed by vacuum distillation. The solvent mixtures (about 1 kg) were gravimetrically prepared. The uncertainty of the balance was smaller than ± 0.4 g.

EXPERIMENTAL RESULTS

The solubility of carbon dioxide (1) in mixtures of water (2) and DMF (3) was measured at DMF mole fractions of the gas-free solvent mixture (x'_3) of about (0.05, 0.1, 0.25, 0.5, 0.75, 0.9, and 1), at temperatures $T \approx$ (314, 354, and 395) K, and total pressures p up to about 10 MPa. The results are given in Table 1

Table 1. Solubility of Carbon Dioxide (1) in DMF (3)[a]

T	m_1	p	$V/\tilde{m}_s$
K	mol·kg^{-1}	MPa	dm^3·kg^{-1}
313.75	0.216 ± 0.001	0.141 ± 0.014	1.1141
313.75	1.65 ± 0.01	0.953 ± 0.014	1.1687
313.75	3.34 ± 0.01	1.78 ± 0.01	1.2431
313.75	5.27 ± 0.02	2.65 ± 0.01	1.3282
313.85	7.21 ± 0.03	3.31 ± 0.01	1.4152
313.15	10.90 ± 0.03	4.19 ± 0.02	1.5725
313.75	13.90 ± 0.03	4.86 ± 0.02	1.7204
313.80	17.80 ± 0.04	5.44 ± 0.02	1.9067
313.80	23.30 ± 0.06	6.05 ± 0.02	2.1769
313.75	31.00 ± 0.08	6.59 ± 0.02	2.5613
354.45	0.959 ± 0.005	1.02 ± 0.01	1.1948
354.40	2.40 ± 0.01	2.37 ± 0.01	1.2582
354.35	3.59 ± 0.01	3.42 ± 0.01	1.3147
354.35	5.04 ± 0.02	4.52 ± 0.02	1.3787
354.40	6.51 ± 0.03	5.45 ± 0.02	1.4462
354.35	8.31 ± 0.03	6.47 ± 0.02	1.5487
354.45	9.96 ± 0.04	7.30 ± 0.02	1.6284
354.40	12.00 ± 0.03	8.09 ± 0.02	1.7368
354.35	14.80 ± 0.04	9.13 ± 0.02	1.8846
394.95	0.578 ± 0.003	0.956 ± 0.014	1.2227
395.00	1.47 ± 0.01	2.28 ± 0.01	1.2639
394.95	1.93 ± 0.01	3.03 ± 0.01	1.2886
395.00	2.77 ± 0.01	4.14 ± 0.02	1.3314
395.00	3.49 ± 0.02	4.99 ± 0.02	1.3713
394.95	3.86 ± 0.02	5.42 ± 0.02	1.3875
395.00	4.58 ± 0.02	6.23 ± 0.02	1.4721
395.10	5.73 ± 0.02	7.30 ± 0.02	1.4978
395.15	6.66 ± 0.02	8.22 ± 0.02	1.5360
394.95	7.70 ± 0.03	9.17 ± 0.02	1.5969

[a]Uncertainty ΔT = ± 0.10 K. m_1 is the molality of CO_2 in the liquid phase (that is, the amount of substance of the gas per kilogram of DMF). $V/\tilde{m}_s$ is the ratio of the cell volume to the mass of the gas-free solvent in the cell.

(for CO_2 in DMF) and in Tables 2 to 4 (for CO_2 in aqueous solutions of DMF). The gas solubility is expressed in terms of molality (m_1), that is, the amount of substance (the number of moles) of the gas per kilogram of (gas-free) solvent. Furthermore the ratio of cell volume V to the mass $\tilde{m}_s$ of the gas-free solvent which was determined as a side-product is also given in those tables. The total pressure above some of those solutions is plotted against the molality of carbon dioxide in Figure 1.

As shown in that figure, a purely physical gas solubility behavior is observed. For "small amounts" of the gas in the

Table 2. Solubility of Carbon Dioxide (1) in Water (2) + DMF (3) at $T \approx 314$ K[a]

T	m_1	p	$V/\tilde{m}_s$	T	m_1	p	$V/\tilde{m}_s$	T	m_1	p	$V/\tilde{m}_s$
K	mol·kg^{-1}	MPa	dm^3·kg^{-1}	K	mol·kg^{-1}	MPa	dm^3·kg^{-1}	K	mol·kg^{-1}	MPa	dm^3·kg^{-1}
	$x'_3 = 0.0500 \pm 0.0001$				$x'_3 = 0.1004 \pm 0.0002$				$x'_3 = 0.2521 \pm 0.0003$		
313.75	0.163 ± 0.001	0.639 ± 0.014	1.0289	313.80	0.173 ± 0.001	0.632 ± 0.014	1.0313	313.70	0.254 ± 0.001	0.688 ± 0.014	1.0407
313.75	0.291 ± 0.001	1.17 ± 0.01	1.0304	313.75	0.303 ± 0.002	1.12 ± 0.01	1.0359	313.95	0.547 ± 0.003	1.47 ± 0.01	1.0523
313.75	0.444 ± 0.002	1.82 ± 0.01	1.0372	313.70	0.407 ± 0.002	1.53 ± 0.01	1.0374	313.70	0.863 ± 0.004	2.32 ± 0.01	1.0628
313.80	0.688 ± 0.003	3.08 ± 0.01	1.0439	313.75	0.622 ± 0.003	2.42 ± 0.01	1.0447	313.80	1.08 ± 0.01	2.91 ± 0.01	1.0758
314.00	0.824 ± 0.004	3.74 ± 0.01	1.0445	313.90	0.886 ± 0.004	3.70 ± 0.01	1.0501	313.95	1.58 ± 0.01	4.31 ± 0.02	1.0910
313.75	0.950 ± 0.005	4.43 ± 0.02	1.0523	313.80	1.03 ± 0.01	4.37 ± 0.02	1.0565	314.05	1.89 ± 0.01	5.19 ± 0.02	1.1068
314.00	1.05 ± 0.01	5.15 ± 0.02	1.0550	313.80	1.31 ± 0.01	6.04 ± 0.02	1.0675	313.75	2.18 ± 0.01	6.09 ± 0.02	1.1123
313.75	1.09 ± 0.01	5.53 ± 0.02	1.0567	313.75	1.52 ± 0.01	7.71 ± 0.02	1.0735	313.75	2.60 ± 0.01	7.37 ± 0.02	1.1317
313.80	1.25 ± 0.01	6.81 ± 0.02	1.0598	313.75	1.59 ± 0.01	8.92 ± 0.02	1.0727	313.70	2.88 ± 0.01	8.99 ± 0.02	1.1371
313.75	1.31 ± 0.01	7.21 ± 0.02	1.0608								
313.75	1.43 ± 0.01	9.15 ± 0.02	1.0622								
	$x'_3 = 0.5029 \pm 0.0006$				$x'_3 = 0.7468 \pm 0.0011$				$x'_3 = 0.8992 \pm 0.0013$		
313.85	0.662 ± 0.003	0.915 ± 0.014	1.0820	313.75	1.01 ± 0.01	0.862 ± 0.014	1.1128	313.70	1.87 ± 0.01	1.20 ± 0.01	1.1738
313.75	2.32 ± 0.01	2.83 ± 0.01	1.1502	313.75	3.78 ± 0.02	2.65 ± 0.01	1.2254	313.65	3.20 ± 0.01	1.90 ± 0.01	1.2308
313.75	3.09 ± 0.01	3.57 ± 0.01	1.1818	313.80	5.52 ± 0.02	3.50 ± 0.01	1.3012	313.75	5.20 ± 0.02	2.89 ± 0.01	1.3197
313.80	5.04 ± 0.02	5.09 ± 0.02	1.2605	313.65	6.79 ± 0.03	4.02 ± 0.01	1.3557	313.75	7.20 ± 0.03	3.60 ± 0.01	1.4050
313.80	6.40 ± 0.03	5.89 ± 0.02	1.3195	313.80	10.40 ± 0.03	5.13 ± 0.02	1.5192	313.75	10.40 ± 0.03	4.47 ± 0.02	1.5532
313.70	7.38 ± 0.03	6.36 ± 0.02	1.3639	313.80	14.00 ± 0.04	5.85 ± 0.02	1.6817	313.65	11.00 ± 0.03	4.62 ± 0.02	1.5840
313.80	9.76 ± 0.03	7.24 ± 0.02	1.4700	313.80	15.70 ± 0.05	6.13 ± 0.02	1.7628	313.75	17.30 ± 0.04	5.71 ± 0.02	1.8807
313.75	12.20 ± 0.03	7.82 ± 0.02	1.5834	313.80	23.00 ± 0.07	6.87 ± 0.02	2.1100	313.75	22.00 ± 0.06	6.23 ± 0.02	2.1105
				313.75	28.50 ± 0.08	7.21 ± 0.02	2.3899	313.75	27.20 ± 0.07	6.63 ± 0.02	2.3678

[a] x'_3 is the mole fraction of DMF on a CO_2 free basis. Uncertainty $\Delta T = \pm 0.10$ K. m_1 is the molality of CO_2 in the liquid phase (that is, the amount of substance of the gas per kilogram of solvent mixture water + DMF). $V/\tilde{m}_s$ is the ratio of the cell volume to the mass of the gas-free solvent in the cell.

dx.doi.org/10.1021/je300105q | J. Chem. Eng. Data 2012, 57, 1249−1266

Table 3. Solubility of Carbon Dioxide (1) in Water (2) + DMF (3) at $T \approx 354$ K[a]

T	m_1	p	$V/\tilde{m}_s$	T	m_1	p	$V/\tilde{m}_s$	T	m_1	p	$V/\tilde{m}_s$
K	mol·kg^{-1}	MPa	dm^3·kg^{-1}	K	mol·kg^{-1}	MPa	dm^3·kg^{-1}	K	mol·kg^{-1}	MPa	dm^3·kg^{-1}
	$x'_3 = 0.0500 \pm 0.0001$				$x'_3 = 0.1004 \pm 0.0002$				$x'_3 = 0.2521 \pm 0.0003$		
354.35	0.131 ± 0.001	0.907 ± 0.014	1.0500	354.35	0.122 ± 0.001	0.719 ± 0.014	1.0580	354.35	0.208 ± 0.001	0.796 ± 0.014	1.0784
354.35	0.203 ± 0.001	1.38 ± 0.02	1.0538	354.35	0.220 ± 0.001	1.27 ± 0.02	1.0620	354.35	0.456 ± 0.002	1.69 ± 0.02	1.0878
354.40	0.360 ± 0.002	2.46 ± 0.02	1.0593	354.35	0.381 ± 0.002	2.20 ± 0.02	1.0670	354.35	0.812 ± 0.004	2.97 ± 0.02	1.1011
354.40	0.460 ± 0.002	3.22 ± 0.02	1.0614	354.35	0.496 ± 0.003	2.88 ± 0.02	1.0712	354.35	0.976 ± 0.005	3.56 ± 0.02	1.1082
354.40	0.596 ± 0.003	4.25 ± 0.02	1.0671	354.35	0.624 ± 0.003	3.69 ± 0.02	1.0752	354.35	1.40 ± 0.01	5.11 ± 0.02	1.1251
354.35	0.759 ± 0.004	5.64 ± 0.02	1.0717	354.35	0.763 ± 0.004	4.58 ± 0.02	1.0802	354.35	1.56 ± 0.01	5.69 ± 0.02	1.1328
354.40	0.850 ± 0.004	6.47 ± 0.02	1.0744	354.35	0.984 ± 0.005	6.11 ± 0.02	1.0854	354.25	1.75 ± 0.01	6.40 ± 0.02	1.1414
354.35	0.982 ± 0.005	7.75 ± 0.02	1.0800	354.35	1.15 ± 0.01	7.40 ± 0.02	1.0949	354.35	2.12 ± 0.01	7.72 ± 0.02	1.1534
354.35	1.155 ± 0.006	9.80 ± 0.02	1.0829	354.35	1.26 ± 0.01	8.41 ± 0.02	1.0955	354.35	2.38 ± 0.01	8.73 ± 0.02	1.1651
				354.35	1.28 ± 0.01	8.60 ± 0.02	1.0954	354.35	2.61 ± 0.01	9.58 ± 0.02	1.1746
				354.35	1.38 ± 0.01	9.52 ± 0.02	1.0998				
	$x'_3 = 0.5029 \pm 0.0006$				$x'_3 = 0.7468 \pm 0.0011$				$x'_3 = 0.8992 \pm 0.0013$		
354.30	0.456 ± 0.002	0.965 ± 0.014	1.1177	354.50	0.909 ± 0.005	1.28 ± 0.01	1.1571	354.40	0.940 ± 0.005	1.09 ± 0.014	1.1881
354.35	1.28 ± 0.01	2.51 ± 0.01	1.1546	354.40	1.81 ± 0.01	2.37 ± 0.01	1.1962	354.40	2.27 ± 0.01	2.57 ± 0.01	1.2464
354.40	1.86 ± 0.01	3.53 ± 0.01	1.1788	354.40	3.45 ± 0.01	4.14 ± 0.02	1.2687	354.35	3.26 ± 0.01	3.44 ± 0.01	1.2930
354.30	2.58 ± 0.01	4.72 ± 0.02	1.2091	354.35	4.20 ± 0.02	4.85 ± 0.02	1.3017	354.35	4.38 ± 0.02	4.40 ± 0.02	1.3476
354.40	3.63 ± 0.01	6.25 ± 0.02	1.2562	354.45	4.30 ± 0.02	4.92 ± 0.02	1.3066	354.15	5.79 ± 0.02	5.40 ± 0.02	1.4155
354.35	4.21 ± 0.02	6.78 ± 0.02	1.2820	354.40	6.53 ± 0.03	6.72 ± 0.02	1.4146	354.40	7.64 ± 0.03	6.57 ± 0.02	1.5077
354.35	4.84 ± 0.02	7.82 ± 0.02	1.3129	354.40	8.18 ± 0.03	7.79 ± 0.02	1.4984	354.40	9.81 ± 0.03	7.71 ± 0.02	1.6190
354.30	5.91 ± 0.02	8.79 ± 0.02	1.3522	354.45	9.61 ± 0.03	8.61 ± 0.02	1.5703	354.40	11.30 ± 0.03	8.32 ± 0.02	1.6957
354.40	6.59 ± 0.03	9.73 ± 0.02	1.3958	354.40	11.0 ± 0.03	9.30 ± 0.02	1.6387	354.40	13.40 ± 0.03	9.11 ± 0.02	1.8046

[a] x'_3 is the mole fraction of DMF on a CO_2 free basis. Uncertainty $\Delta T = \pm 0.10$ K. m_1 is the molality of CO_2 in the liquid phase (that is, the amount of substance of the gas per kilogram of solvent mixture water + DMF). $V/\tilde{m}_s$ is the ratio of the cell volume to the mass of the gas-free solvent in the cell.

dx.doi.org/10.1021/je300105q | J. Chem. Eng. Data 2012, 57, 1249−1266

Table 4. Solubility of Carbon Dioxide (1) in Water (2) + DMF (3) at $T \approx 395$ K[a]

T	m_1	p	$V/\tilde{m}_s$	T	m_1	p	$V/\tilde{m}_s$	T	m_1	p	$V/\tilde{m}_s$
K	mol·kg^{-1}	MPa	dm^3·kg^{-1}	K	mol·kg^{-1}	MPa	dm^3·kg^{-1}	K	mol·kg^{-1}	MPa	dm^3·kg^{-1}
	$x'_3 = 0.0500 \pm 0.0001$				$x'_3 = 0.1004 \pm 0.0002$				$x'_3 = 0.2521 \pm 0.0003$		
395.00	0.105 ± 0.001	1.05 ± 0.01	1.0853	394.90	0.117 ± 0.001	0.968 ± 0.014	1.1073	394.95	0.207 ± 0.001	1.037 ± 0.014	1.1264
395.00	0.185 ± 0.001	1.66 ± 0.01	1.0879	394.90	0.189 ± 0.001	1.44 ± 0.01	1.1000	394.95	0.377 ± 0.002	1.75 ± 0.01	1.1327
395.00	0.289 ± 0.002	2.58 ± 0.01	1.0910	394.95	0.303 ± 0.002	2.22 ± 0.01	1.1041	394.95	0.609 ± 0.003	2.70 ± 0.01	1.1423
395.00	0.400 ± 0.002	3.55 ± 0.01	1.0953	394.95	0.418 ± 0.002	2.99 ± 0.01	1.1088	395.00	0.806 ± 0.004	3.50 ± 0.01	1.1519
395.00	0.519 ± 0.003	4.63 ± 0.02	1.0985	395.00	0.654 ± 0.003	4.65 ± 0.02	1.1158	395.00	1.04 ± 0.01	4.47 ± 0.02	1.1621
395.00	0.628 ± 0.003	5.67 ± 0.02	1.1026	395.00	0.887 ± 0.004	6.37 ± 0.02	1.1263	394.95	1.32 ± 0.01	5.63 ± 0.02	1.1753
394.95	0.709 ± 0.004	6.44 ± 0.02	1.1037	395.00	1.14 ± 0.01	8.13 ± 0.02	1.1342	395.00	1.59 ± 0.01	6.70 ± 0.02	1.1869
394.95	0.852 ± 0.004	7.90 ± 0.02	1.1108	394.95	1.25 ± 0.01	9.02 ± 0.02	1.1357	395.00	1.78 ± 0.01	7.37 ± 0.02	1.1947
395.00	0.992 ± 0.005	9.48 ± 0.02	1.1150	395.00	1.35 ± 0.01	10.2 ± 0.02	1.1417	395.00	2.02 ± 0.01	8.39 ± 0.02	1.2051
								395.00	2.28 ± 0.01	9.41 ± 0.02	1.2159
	$x'_3 = 0.5029 \pm 0.0006$				$x'_3 = 0.7468 \pm 0.0011$				$x'_3 = 0.8992 \pm 0.0013$		
394.95	0.367 ± 0.002	1.09 ± 0.01	1.1676	395.00	0.445 ± 0.002	0.952 ± 0.014	1.1895	395.05	0.560 ± 0.003	1.01 ± 0.01	1.2259
395.00	0.598 ± 0.003	1.67 ± 0.01	1.1797	394.90	0.946 ± 0.005	1.88 ± 0.01	1.2138	394.95	1.32 ± 0.01	2.21 ± 0.01	1.2597
394.90	1.38 ± 0.01	3.52 ± 0.01	1.2168	395.00	1.63 ± 0.01	3.06 ± 0.01	1.2434	395.25	2.13 ± 0.01	3.50 ± 0.01	1.3040
394.95	1.78 ± 0.01	4.32 ± 0.02	1.2346	394.95	2.02 ± 0.01	3.72 ± 0.01	1.2614	395.00	2.79 ± 0.01	4.40 ± 0.02	1.3361
394.90	2.32 ± 0.01	5.59 ± 0.02	1.2583	394.95	2.87 ± 0.02	5.01 ± 0.02	1.3070	395.20	3.57 ± 0.01	5.41 ± 0.02	1.3788
394.95	2.71 ± 0.01	6.38 ± 0.02	1.2745	395.00	3.57 ± 0.01	6.00 ± 0.02	1.3427	395.00	4.50 ± 0.02	6.45 ± 0.02	1.4266
395.00	3.31 ± 0.01	7.51 ± 0.02	1.3069	394.90	4.44 ± 0.02	7.13 ± 0.02	1.3885	394.95	4.83 ± 0.02	6.83 ± 0.02	1.4457
395.00	3.87 ± 0.02	8.52 ± 0.02	1.3370	395.00	4.70 ± 0.02	7.47 ± 0.02	1.3999	395.00	5.59 ± 0.02	7.65 ± 0.02	1.4877
395.05	4.46 ± 0.02	9.52 ± 0.02	1.3654	394.95	5.75 ± 0.02	8.65 ± 0.02	1.4580	394.95	6.54 ± 0.03	8.49 ± 0.02	1.5391
				395.00	6.40 ± 0.03	9.36 ± 0.02	1.4926	394.95	7.25 ± 0.03	9.21 ± 0.02	1.5799

[a] x'_3 is the mole fraction of DMF on a CO_2 free basis. Uncertainty $\Delta T = \pm 0.10$ K. m_1 is the molality of CO_2 in the liquid phase (that is, the amount of substance of the gas per kilogram of solvent mixture water + DMF). $V/\tilde{m}_s$ is the ratio of the cell volume to the mass of the gas-free solvent in the cell.

dx.doi.org/10.1021/je300105q | J. Chem. Eng. Data 2012, 57, 1249−1266

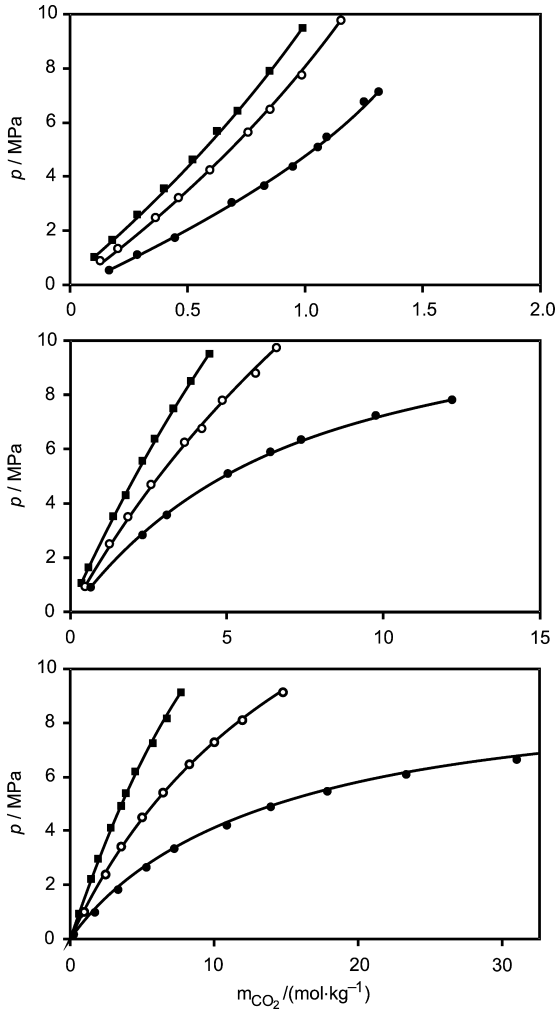

Figure 1. Experimental results for the total pressure p above solutions of CO_2 (1) + H_2O (2) + DMF (3) plotted against the molality of CO_2 in the liquid phase (that is, the amount of substance of the gas per kilogram of solvent mixture H_2O + DMF): ●, $T \approx 314$ K; ○, $T \approx 354$ K; ■, $T \approx 395$ K. The mole fraction of DMF x'_3 in the gas-free solvent is $x'_3 \approx 0.05$ (top), $x'_3 \approx 0.5$ (middle), and $x'_3 = 1$ (down).

liquid, and according to Henry's law, the solubility pressure practically linearly increases with increasing amount of dissolved gas. For "higher amounts" of the gas in the liquid, that linearity turns into a more or less pronounced curvature which is due to the influence of pressure on Henry's law constant (of CO_2 in the solvents) and to the physical interactions between the gas molecules in the liquid mixture as well as in the vapor phase.

As expected, the solubility of carbon dioxide is much higher in DMF and in the DMF-rich aqueous solutions than it is in water. For example, at $T = 354$ K and $p = 4$ MPa, about $m_1 =$ (0.57, 0.66, 1.1, 2.2, 3.4, 4.4, and 4.5) moles of CO_2 are dissolved in 1 kg of the solvent with a composition of $x'_3 =$ (0.05, 0.1, 0.25, 0.5, 0.75, 0.9, and 1), respectively. In addition, and throughout the range of solvent mixture composition, the solubility of carbon dioxide (on the molality scale) decreases with rising temperature. For example, at $p = 4$ MPa and $x'_3 =$ (0.05, 0.1, 0.25, 0.5, 0.75, 0.9, and 1), $m_1 \approx$ (0.87, 0.95, 1.5, 3.6, 6.7, 8.7, and 10) mol·kg^{-1} at $T = 314$ K and $m_1 \approx$ (0.45, 0.56, 0.93, 1.6, 2.2, 2.5, and 2.7) mol·kg^{-1} at $T = 395$ K.

COMPARISON OF EXPERIMENTAL RESULTS WITH LITERATURE DATA

Experimental results for the solubility of CO_2 in DMF have been published by Melzer et al.[82] (at temperatures between (213 and 298) K), Schlichting[83] (at temperatures between (293 and 338) K), Chang et al.[84] (at (291, 301, and 310) K), Duran-Valencia et al.[89] (at (294, 313, and 338) K), Byun et al.[90] (at (318, 338, 358, 378, and 398) K), and Liu et al.[91] (at (323, 323, 333, 343, and 353) K).

A comparison between the results of Chang et al. (for 310 K), Duran-Valencia et al. (for 313.05 K), and the present work (for 313.8 K) is shown in Figure 2. The experimental results by

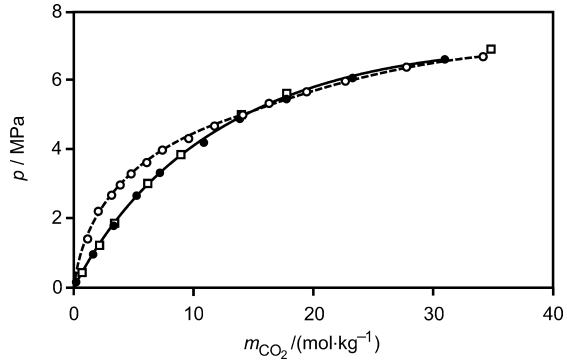

Figure 2. Experimental results for the solubility of CO_2 in DMF: ○, Chang et al.[84] for $T = 310.1$ K; □, Duran-Valencia et al.[89] for $T = 313.05$ K; ●, this work for $T \approx 314$ K.

Duran-Valencia et al. nicely agree with the experimental results of the present work. The differences in the solubility pressure are typically about 3 %, but there is a systematic deviation as at low (high) pressures the experimental results of Duran-Valencia et al. for the solubility pressure are systematically below (above) the results of the current investigation. A comparison between the correlation results of the present work and the experimental results of Duran-Valencia et al.[89] (at 294 and 338 K) is given below. The experimental results for the solubility pressure reported by Chang et al. (for 310 K) agree with the results of the current investigation within experimental uncertainty only at pressures above 5 MPa ($m_{CO_2} > 15$ mol·kg^{-1}). At those high pressures the liquid phase contains a large amount of CO_2 (for example, at $m_{CO_2} \approx 30$ mol·kg^{-1} the mole fraction of CO_2 in the liquid mixture of (DMF + CO_2) amounts to nearly 0.7). At lower pressures the experimental results reported by Chang et al. for the total pressure surmount the new experimental results. The largest relative deviations (relative deviations of more than 50 %) are observed around $m_{CO_2} \approx$ (2 to 4) mol·kg^{-1}. This observation might be explained by the presence of another gas in the measurements by Chang et al. That gas should be sparsely soluble in DMF but well soluble in liquid CO_2. That assumption is also supported by the comparisons described below for Henry's constant (from Melzer et al.[82]) and the volumetric properties from Chang et al.[84]

The phase equilibrium investigations by Byun at al.[90] as well as by Liu et al.[91] are restricted to liquid mixtures with rather high mole fractions of CO_2 ($x_{CO_2} > 0.2$). Therefore, there is only a small range of overlapping with the results of the present investigation. As a typical example, Figure 3 shows the experimental results for the solubility pressure by Byun et al. (for 358 K) as well as by Liu et al. (for 353 K) in comparison with the

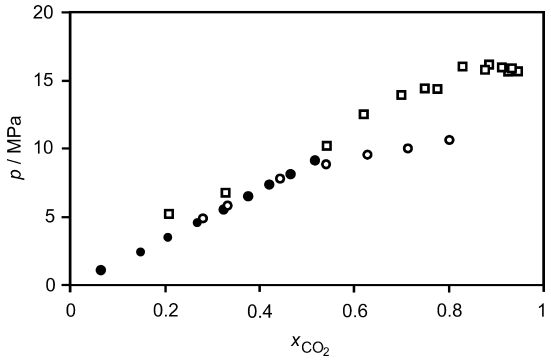

Figure 3. Experimental results for the solubility of CO_2 in DMF: ○, Liu et al.[91] for T = 353 K; □, Byun et al.[90] for T = 358 K; ●, this work for $T \approx 354$ K.

experimental results of the present investigation (for 354 K). The results reported by Liu et al.[91] agree with the results of the present investigation within about 4 %, whereas the experimental results for the solubility pressure reported by Byun et al.[90] systematically deviate from the results from both other investigations. The deviations from the results of the present work increase with a decreasing concentration of CO_2 to 32 % at x_{CO_2} = 0.21. Calculations with the model described below showed that such a large deviation cannot be caused by the difference in temperature (i.e., ≈ 4 K) between both investigations. At lower temperatures the deviations between the experimental results reported by Byun et al. (for 318 K) and those of the present investigation (for 314 K) are larger (max. deviation about 50 %), whereas at higher temperatures, (395 and 398) K, the deviations are smaller (maximum deviation about 5 %).

Melzer et al.[82] also reported experimental results for the solubility of carbon dioxide in aqueous solutions of DMF at x'_3 > 0.5, but they reported only Henry constants. Their results are compared with the results of the present investigation below.

EVALUATION OF HENRY'S CONSTANT OF CO_2 IN DMF AND IN AQUEOUS SOLUTIONS OF DMF

The (molality scale based) zero-pressure Henry's constant of CO_2 in liquid DMF as well as in aqueous solutions of DMF $k^{m,0}_{H,CO_2,s}(T, x'_3)$ was determined from the well-known extrapolation procedure (at constant temperature and solvent composition):

$$k^{m,0}_{H,CO_2,s}(T, x'_3) = \lim_{p\to 0}\left[\frac{f_1(T, p, y_j)}{(m_1/m^\circ)}\right] \tag{1}$$

where m° is the unit of molality (m° = 1 mol·kg^{-1}) and:

$$f_1(T, p, y_j) = y_1 p \phi_1(T, p, y_j) \tag{2}$$

f_1 and ϕ_1 are the fugacity and the fugacity coefficient of carbon dioxide, respectively, and y_j is the mole fraction of component j (j = 1, 2, 3) in the vapor.

To evaluate the fugacity of carbon dioxide in the vapor phase above the liquid mixtures of (CO_2 + H_2O + DMF), which is utilized in eq 1, one requires information on the vapor-phase composition. The vapor-phase composition was estimated for each experimental point (at given temperature, liquid phase composition, and solubility pressure) from the extended Raoult's law (cf., eq 3) for each of the solvent components i in an iterative procedure (cf., ref 67).

$$p_i^{sat}\phi_i^{sat}\exp\left[\frac{v_i(p - p_i^{sat})}{RT}\right]a_i = y_i p \phi_i \qquad (i = 2, 3) \tag{3}$$

where p_i^{sat} and ϕ_i^{sat} are saturation properties (vapor pressure, fugacity coefficient) and v_i is the molar liquid volume of a pure solvent component i. R is the universal gas constant, and a_i is the activity of solvent component i in the liquid phase. The activity a_i of a solvent component i in the liquid mixture of (CO_2 + H_2O + DMF) or (CO_2 + DMF) was estimated from (see also Pérez-Salado Kamps[67] and the modeling section below):

$$a_i = x_i \gamma_i(T, x'_3)\gamma_{i,conv}(T, x'_3, m_1) \qquad (i = 2, 3) \tag{4}$$

x_i is the true mole fraction of solvent component i in the liquid mixture of (CO_2 + H_2O + DMF):

$$x_i = \frac{x'_i}{1 + (m_1/m^\circ)M_s^*} \qquad (i = 2, 3) \tag{5}$$

where M_s^* is the (mean) relative molar mass of the solvent divided by 1000. For the binary solvent mixture under consideration it is

$$M_s^* = M_2^* + x'_3(M_3^* - M_2^*) \tag{6}$$

where M_2^* = 0.018015 (for water) and M_3^* = 0.0731 (for DMF).

$\gamma_i(T, x'_3)$ is the activity coefficient of solvent component i in the gas-free solvent. For pure DMF (as the solvent), that is, when x'_3 = 1:

$$\gamma_i(T, x'_3 = 1) = 1 \tag{7a}$$

whereas in aqueous solutions of DMF (as the solvent) $\gamma_i(T,x'_3)$ was approximated with the universal quasichemical activity coefficent (UNIQUAC) model

$$\gamma_i(T, x'_3) = \gamma_{i,UNIQUAC}(T, x'_3) \qquad (i = 2, 3) \tag{7b}$$

$\gamma_{i,conv}(T,x'_3,m_1)$ is the so-called conversion term, which in a first approximation accounts for the presence of the solute gas (cf., ref 67):

$$\ln \gamma_{i,conv} = -\left(\frac{m_1}{m^\circ}\right)M_s^* + \ln\left[1 + \left(\frac{m_1}{m^\circ}\right)M_s^*\right] \qquad (i = 2, 3) \tag{8}$$

For each experimental data point (composition of the gas-free solvent, temperature, pressure, and molality of CO_2 in the liquid phase) eq 3 was solved in an iterative procedure to determine an estimate for the composition of the vapor phase. This procedure requires several properties:

- vapor pressure and the molar volume of the liquid solvent components,
- fugacity coefficient of a pure solvent component at saturation,
- UNIQUAC parameters for solvent components, and
- fugacity coefficients of all components in the vapor phase.

dx.doi.org/10.1021/je300105q | J. Chem. Eng. Data 2012, 57, 1249−1266

The vapor pressure of pure water (p_2^{sat}) and the molar volume of saturated liquid water (v_2) were calculated from the correlation equations given by Saul and Wagner.[73] Numerical values for the vapor pressure of DMF (p_3^{sat}) and liquid phase molar volumes (v_3) were taken from the Detherm data collection[74] and correlated as a function of temperature (cf., Table 5).

Table 5. Properties of Saturated Liquid DMF

(a) Vapor pressure p_3^{sat}

$$\ln\left(\frac{p_3^{sat}}{p_{c,3}}\right) = \frac{T_{c,3}}{T}(-6.879\Theta + 0.260\Theta^{1.5} - 5.474\Theta^3 + 7.953\Theta^6)$$

$p_{c,3}$ (= 4.357 MPa) and $T_{c,3}$ (= 643.15 K) are the critical pressure and the critical temperature of DMF,[74] respectively; $\Theta = 1 - (T/T_{c,3})$.

(b) Molar volume v_3

$$\frac{v_3}{\mathrm{dm^3 \cdot mol^{-1}}} = \frac{1000}{16.846 - 0.01315(T/\mathrm{K})}$$

The fugacity coefficients ϕ_i (and ϕ_i^{sat}) are calculated from the virial equation of state which was truncated after the second virial coefficient. Pure component second virial coefficients $B_{i,i}$ for CO_2 and water are calculated from a correlation based on experimental data compiled by Dymond and Smith.[75] Details for the calculation of the second virial coefficients of all pure components are given in Table 6. Mixed second virial coefficients $B_{i,j}$

Table 6. Pure Component Second Virial Coefficients $B_{i,i}$

$$\frac{B_{i,i}}{\mathrm{cm^3 \cdot mol^{-1}}} = a_i + b_i\left[\frac{c_i}{(T/\mathrm{K})}\right]^{d_i}$$

i	a_i	b_i	c_i	d_i	T/K
CO_2	65.703	−184.854	304.16	1.36	273−573
H_2O	−53.527	−39.287	647.3	4.277	373−577
DMF	−221.7	−598.14	500	3.6	300−430

are calculated as proposed by Hayden and O'Connell.[76] Pseudocritical temperatures and pressures ($T_{c,i}$, $p_{c,i}$), molecular dipole moments (μ_i), and mean radii of gyration ($R_{D,i}$) of the pure components as well as association parameters (η_{ij}) were taken from refs 6, 74, and 76 (cf. Table 7).

Table 7. Parameters for the Hayden and O'Connell Method for Estimating Mixed Second Virial Coefficients

(a) Pure Component Parameters (Critical Temperature $T_{c,i}$, Critical Pressure $p_{c,i}$, Dipole Moment μ_i, and Radius of Gyration $R_{D,i}$)

	$T_{c,i}$	$p_{c,i}$	μ_i	$R_{D,i}$
i	K	MPa	10^{-30} Cm	10^{-10} m
CO_2	241.0	5.38	0	0.9918
H_2O	647.3	22.13	6.10	0.615
DMF	643.15	4.357	12.7	2.74

(b) Parameter η_{ij} for Association between Molecules i and j

η_{ij}	CO_2	H_2O	DMF
CO_2	0.16	0.3	0
H_2O	0.3	1.7	0
DMF	0	0	0

The UNIQUAC size and surface parameters of water and DMF were calculated according to Bondi.[77] Interaction parameters were adjusted to vapor−liquid equilibrium data for that binary system (for details see Jödecke[78]). All UNIQUAC parameters are given in Table 8.

Table 8. UNIQUAC Parameters for (DMF + Water)[78]

(a) Size (r_i) and Surface Parameters (q_i)

i	r_i	q_i
H_2O	0.92	1.40
DMF	3.086	2.736

(b) Interaction Parameters ($\tau_{DMF,water}$ and $\tau_{water,DMF}$)

$$\tau_{i,j} = \exp\left(a_{i,j} + \frac{b_{i,j}}{T/\mathrm{K}}\right)$$

	$a_{i,j}$	$b_{i,j}$
$\tau_{DMF,water}$	1.2563	−410.38
$\tau_{water,DMF}$	−2.3525	875.64

An estimation based on the method described above for the solubility of CO_2 in pure DMF proved that the mole fraction of DMF in the vapor phase at the lowest pressure is about 0.008, 0.08, and 0.04 for the experimental data at (314, 354, and 395) K, respectively. With increasing pressure that mole fraction decreases further. Therefore, a second extrapolation of the experimental data was performed for the evaluation to determine Henry's constant of CO_2 in DMF, where the vapor phase was treated as pure carbon dioxide and the fugacity of CO_2 was calculated from the *Thermofluids* Software.[79] At low (high) pressures numbers for $f_1/(m_1/m^\circ)$ calculated with the virial equation are somewhat lower (higher) than the results which follow from the assumption that the vapor phase is pure carbon dioxide.

As a typical example, Figure 4 shows the extrapolation to determine Henry's constant of CO_2 in pure DMF at 354 K.

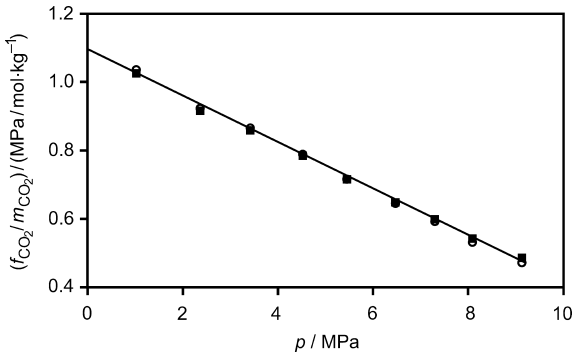

Figure 4. Extrapolation to determine Henry's constant of CO_2 in DMF at $T \approx 354$ K with different assumptions about the vapor phase: ○, vapor phase is treated as pure CO_2; ■, fugacity of CO_2 in the vapor phase is calculated with the virial equation of state (truncated after the second virial coefficient).

Figure 5 shows an example for the extrapolation when the solvent is an aqueous solution of DMF. At higher temperatures (i.e., at 395 K), low mole fractions of DMF in the aqueous solvent (for example, at $x'_3 = 0.05$ in the gas-free solvent mixture), and low total pressures, the partial pressure of water contributes significantly to the total pressure. In that range the assumption that the vapor phase consists of pure carbon dioxide results in large errors for Henry's constant. Therefore, all extrapolations were based on the results obtained from the virial equation of state.

dx.doi.org/10.1021/je300105q | J. Chem. Eng. Data 2012, 57, 1249−1266

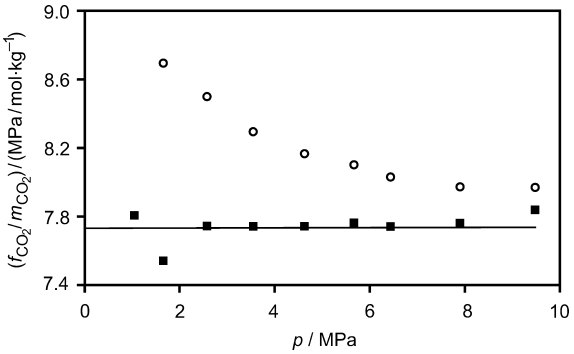

Figure 5. Extrapolation to determine the Henry's constant of CO_2 in aqueous solutions of DMF ($x'_3 \approx 0.05$) at $T \approx 395$ K with different assumptions about the vapor phase: ○, vapor phase is treated as pure CO_2; ■, fugacity of CO_2 in the vapor phase is calculated with the virial equation of state (truncated after the second virial coefficient).

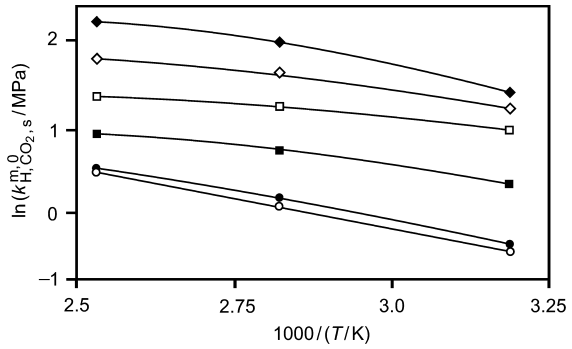

Figure 6. Henry's constant of CO_2 in aqueous solutions of DMF: ♦, $x'_3 = 0$ (from Rumpf and Maurer[6]); ◊, $x'_3 \approx 0.1$; □, $x'_3 \approx 0.25$; ■, $x'_3 \approx 0.5$; ●, $x'_3 \approx 0.75$; ○, $x'_3 = 1.0$.

The uncertainty of Henry's constant (resulting from the uncertainty of the experimental results and the extrapolation procedure) is estimated to be less than ± 2 %. The (molality scale based) Henry's constant of CO_2 in DMF is by about a factor of 6 smaller (the solubility of CO_2 in DMF—on a molality scale basis—is about a factor of 6 larger) than that of CO_2 in water. The results are given in Table 9 and shown in Figure 6 as $\ln k^{m,0}_{H,CO_2,s}$ over the reciprocal temperature.

For pure DMF the experimental results can be well-correlated by a linear relation between $\ln k^{m,0}_{H,CO_2,s}$ and the reciprocal temperature. However, with increasing mole fraction of water in the solvent, an increasing curvature of that plot is observed. The following equation was selected to correlate the influence of temperature on Henry's constant of CO_2 in aqueous solutions of DMF:

$$\ln(k^{m,0}_{H,CO_2,s}/\mathrm{MPa}) = a(x'_3) + b(x'_3)\cdot\frac{1000}{T/\mathrm{K}} + f(x'_3)\cdot[C_W \ln(T/\mathrm{K}) + D_W(T/\mathrm{K})] \quad (9)$$

Parameters C_W (= −28.7488) and D_W (= 0.0144074) are taken from the correlation of Rumpf et al.[6] for Henry's constant of CO_2 in water and $f(x'_3)$ is an empirical factor that accounts for the decreasing curvature of a plot of Henry's constant versus the reciprocal temperature when the mole fraction of DMF in the gas-free solvent mixture x'_3 increases. That empirical factor was chosen to fulfill the following conditions:

$$f(x'_3) \to 1 \quad \text{for} \quad x'_3 \to 0 \quad \text{(i.e., for pure water)}$$

$$f(x'_3) \to 0 \quad \text{for} \quad x'_3 \to 1 \quad \text{(i.e., for pure DMF)}$$

A simple function that fulfills both conditions is:

$$f(x'_3) = 1 + x'_3(dx'_2 - 1) \quad (10)$$

where d is treated as an adjustable parameter.

Parameters $a(x'_3)$, $b(x'_3)$, and d were fit to the new experimental data for Henry's constant for CO_2 in DMF and aqueous solutions of DMF. The resulting parameters are given in Table 10. The correlation results agree with the experimentally determined Henry's constants with a standard deviation of less than 3 % and a maximum deviation of 6.3 % (at 354.4 K and $x'_3 = 0.75$).

The influence of the solvent composition on Henry's constant of CO_2 is shown in Figure 7.

Adding some DMF to water results in a rather large decrease of Henry's constant, whereas vice versa, adding some water to DMF results only in a small increase of the Henry's constant at all investigated temperatures. The strong influence of small amounts of DMF in water on Henry's constant of CO_2 is most obvious at higher temperatures. The experimental results for Henry's constant of CO_2 in (H_2O + DMF) were correlated using the following equation that combines a simple mixing rule

Table 9. Henry's Constant $k^{m,0}_{H,CO_2,s}$ (at Zero Pressure on the Molality Scale) and Partial Molar Volume $V^{\infty}_{m,CO_2,s}$ of CO_2 (1) in Solvent Mixtures of H_2O (2) + DMF (3)

	T = (313.8 ± 0.1) K		T = (354.4 ± 0.1) K		T = (395.0 ± 0.1) K	
	$k^{m,0}_{H,CO_2,s}$	$V^{\infty}_{m,CO_2,s}$	$k^{m,0}_{H,CO_2,s}$	$V^{\infty}_{m,CO_2,s}$	$k^{m,0}_{H,CO_2,s}$	$V^{\infty}_{m,CO_2,s}$
x'_3[a]	MPa	cm³·mol⁻¹	MPa	cm³·mol⁻¹	MPa	cm³·mol⁻¹
1	0.617	45.1	1.095	48.3	1.617	53.1
0.8992	0.690	45.8	1.203	48.7	1.714	52.2
0.7468	0.892	44.4	1.461	46.9	1.955	50.0
0.5029	1.417	42.5	2.115	43.5	2.598	46.4
0.2521	2.688	38.4	3.620	40.1	4.080	44.2
0.1004	3.570	30.5	5.448	32.8	6.437	35.1
0.0500	3.819	28.4	6.746	31.6	7.732	31.5
0[b]	4.289	33.0	7.824	36.0	10.13	41.0

[a] x'_3 is the mole fraction of DMF on CO_2 free basis. [b] Henry's constant adopted from ref 6, partial molar volume calculated according to Brelvi and O'Connell.[80]

dx.doi.org/10.1021/je300105q | J. Chem. Eng. Data 2012, 57, 1249−1266

Table 10. Correlation[a] for the Influence of Temperature on Henry's Constant $k^{m,0}_{H,CO_2,s}$

$$\ln(k^{m,0}_{H,CO_2,s}/\mathrm{MPa}) = a(x'_3) + b(x'_3)\frac{1000}{T/\mathrm{K}} + f(x'_3)(C_W \ln(T/\mathrm{K}) + D_W(T/\mathrm{K}))$$

x'_3[b]	$a(x'_3)$	$b(x'_3)$
1	4.23005	−1.47579
0.8992	−27.43368	0.00240
0.7468	−53.98950	1.35496
0.5029	−42.58988	1.10090
0.2521	38.23218	−2.20665
0.1004	122.35191	−6.14677
0.0500	156.27034	−7.80627
0	192.876[c]	−9.62441[c]

[a] $C_W = -28.7488$ and $D_W = 0.0144074$ and $f(x'_3) = 1 + x'_3(2.97025x'_2 - 1)$. [b] x'_2 and x'_3 are the mole fractions (on CO_2-free basis) of water and DMF, respectively. [c] From Rumpf et al.[6]

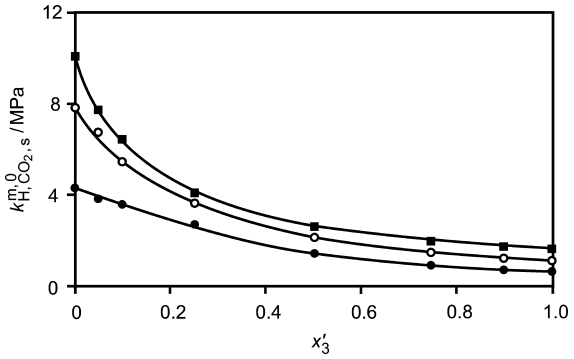

Figure 7. Influence of the mole fraction of DMF x'_3 in the gas-free solvent on the Henry's constant of CO_2 in aqueous solutions of DMF: ■, $T \approx 314$ K; ○, $T \approx 354$ K; ●, $T \approx 395$ K.

(i.e., ideal mixture) for $\ln k^{m,0}_{H,CO_2,s}$ with an expression similar to the Redlich–Kister equation (cf., ref 67):

$$\ln(k^{m,0}_{H,CO_2,s}/\mathrm{MPa}) = \ln(k^{m,0}_{H,CO_2,W}/\mathrm{MPa}) + x'_3[\ln(k^{m,0}_{H,CO_2,DMF}/\mathrm{MPa}) - \ln(k^{m,0}_{H,CO_2,W}/\mathrm{MPa})] + x'_2x'_3[A_{H,0}(T) + (x'_3 - x'_2)A_{H,1}(T) + (x'_3 - x'_2)^2A_{H,2}(T)] \quad (11)$$

where $k^{m,0}_{H,CO_2,W}$ and $k^{m,0}_{H,CO_2,DMF}$ are the Henry's constants for the solubility of CO_2 in water and DMF, respectively, which were taken from Rumpf et al.[6] and the present work (cf. eq 9 and parameters in Table 10 for $x'_3 = 1$). Parameters $A_{H,0}(T)$, $A_{H,1}(T)$, and $A_{H,2}(T)$ were fit to the experimental results for the influence of the composition of the solvent mixture on Henry's constant. The results are given in Table 11. The correlation equations reproduce the experimental results for $k^{m,0}_{H,CO_2,s}$ at 314 K (354.4 K, 395.0 K) with a standard deviation of 2.2 % (1.7 %, 1.0 %). At 314 K (354.4 K, 395 K) the maximum deviation amounts to 3.2 % at $x'_3 = 0.5$ (3.5 % at $x'_3 = 0.05$, 2.4 % at $x'_3 = 0.05$).

Table 11. Correlation for the Influence of Solvent Composition on Henry's Constant $k^{m,0}_{H,CO_2,s}$ (cf., eq 11) and on the Partial Molar Volume $V^{\infty}_{m,CO_2,s}$ (cf., eq 15)

T/K	314.0	354.4	395.0
$A_{H,0}$	−0.39981	−1.24173	−1.73856
$A_{H,1}$	−0.68109	0.36626	0.98525
$A_{H,2}$	0	−0.29568	−0.78375
$V^{\infty}_{m,CO_2,W}/(\mathrm{cm^3\cdot mol^{-1}})$	22.89	25.90	26.20
	all temperatures		
$A_{V,0}$	31.32		
$A_{V,1}$	23.32		
$A_{V,2}$	33.87		

COMPARISON WITH LITERATURE DATA FOR HENRY'S CONSTANT

Melzer et al.[82] reported experimental results for Henry's constant (on the mole fraction scale) of CO_2 in pure DMF and aqueous solutions of DMF ($x'_3 > 0.5$) at temperatures between (213 and 298) K, that is, at temperatures below the scope of the present investigation. Schlichting[83] used the same equipment and determined Henry's constant of CO_2 in DMF at approximately (293.2, 313.1, and 338.1) K. Both data sets give Henry's constant on mole fraction scale $k^{x}_{H,CO_2,s}$. These data were converted to the molality scale based Henry's constant $k^{m,0}_{H,CO_2,s}$ (neglecting the influence of pressure on $k^{x}_{H,CO_2,s}$):

$$k^{m,0}_{H,CO_2,s} = k^{x}_{H,CO_2,s}\cdot M^*_s \quad (12)$$

where M^*_s is given by eq 6. Equation 9 (with parameters given in Table 10) was used to extrapolate the results of the present work to lower temperatures. For pure DMF, at 298 K the relative difference between the correlation results from eq 9 and the data from Melzer et al. is below 0.1 %. This is well below the experimental uncertainty of the data by Melzer et al. (which is at least 1.6 %). However, with further decreasing temperature the difference between the correlation equation and the results of Melzer et al. increases (for example 8.4 % at 274 K and nearly 20 % at 253 K). Schlichting's results for Henry's constant deviate from the correlation given by eq 9 by 5 % (at 293 K), 0.4 % at (313 K), and 2 % (at 338 K); that is, the deviations are larger than the experimental uncertainty only at 293 K. We assume that these larger deviations at low temperatures are caused by the failure of eq 9 to give reliable estimates at those low temperatures.

However, the good agreement in the temperature range from (293 to 338) K confirms the above-mentioned suspicion for the reason for the large deviations between the new results and those of Chang et al. for the total pressure above (DMF + CO_2) at 310 K.

The set of Henry's constant from Melzer et al., from Schlichting, and from the present work was used to find the following correlation for Henry's constant of CO_2 in DMF for temperatures between (213 and 395) K:

$$\ln(k^{m,0}_{H,CO_2,DMF}/\mathrm{MPa}) = 0.99471 - \frac{2093.54}{T/\mathrm{K}} + 1.41601\ln(T/\mathrm{K}) - 0.0093386(T/\mathrm{K}) \quad (13)$$

dx.doi.org/10.1021/je300105q | J. Chem. Eng. Data 2012, 57, 1249–1266

This equation describes the experimental data with a standard deviation of 1.7 % and a maximum deviation (at 233 K) of 3.2 %.

For aqueous solutions with $x'_3 = 0.9$ (and 0.5) the deviations between the extrapolation results from eq 9 and the data reported by Melzer et al. increase to 3 % (and 8 %) at 298 K and to about 20 % (and 36 %) at 253 K.

EVALUATION OF THE PARTIAL MOLAR VOLUME OF CO_2 AT INFINITE DILUTION IN DMF AND IN AQUEOUS SOLUTIONS OF DMF

The experimental results for the ratio of cell volume V and mass of (gas-free) solvent $\tilde{m}_s$ were used to determine the partial molar volume of CO_2 at infinite dilution in the solvent $V^{\infty}_{m,CO_2,s}$. At low gas molalities, the following relation holds for the influence of gas molality m_{CO_2} on $V/\tilde{m}_s$ at (T, x'_3) = constant (cf. ref 81):

$$\frac{V}{\tilde{m}_s} = \frac{1}{\rho_s} + m_{CO_2} \cdot V^{\infty}_{m,CO_2,s} \tag{14}$$

where ρ_s is the density of the (gas-free) solvent. As a typical example, Figure 8 shows a plot of the experimental results

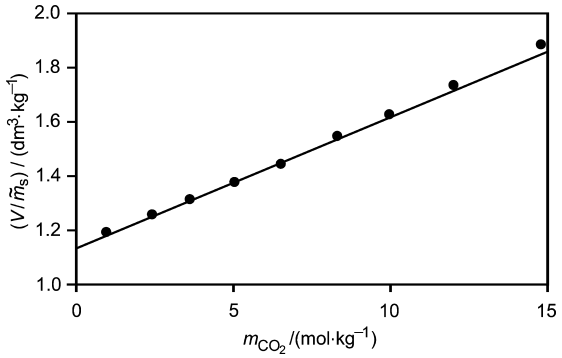

Figure 8. Extrapolation to determine the partial molar volume of CO_2 at infinite dilution in DMF at $T \approx 354$ K.

for $V/\tilde{m}_s$ versus m_{CO_2} (when CO_2 is dissolved in pure DMF at 354 K).

The linear behavior ($V/\tilde{m}_s$ versus m_{CO_2}) prevails up to large gas molalities. Therefore—although the estimated uncertainty of the reported experimental results for $V/\tilde{m}_s$ is about 0.4 %—the partial molar volume $V^{\infty}_{m,CO_2,s}$ can be reliably determined. We estimate that the absolute uncertainty in the results for $V^{\infty}_{m,CO_2,s}$ is below ± 5 cm^3·mol^{-1}. These results are summarized in Table 9 and shown in Figure 9 together with the prediction results from the method of Brelvi and O'Connell[80] for the partial molar volume of CO_2 in pure water (setting the characteristic molar volume of CO_2 and H_2O in that method to (80 and 46.4) cm^3·mol^{-1}, respectively). The partial molar volume of CO_2 at infinite dilution in DMF decreases from about 53 cm^3·mol^{-1} to about 45 cm^3·mol^{-1} when the temperature decreases from (395 to 314) K. These values correspond to a volume expansion of about 40 % when 10 mol of CO_2 are dissolved in pure DMF at about 350 K (i.e., at a pressure of about 8 MPa). The partial molar volume of CO_2 also decreases at constant temperature with increasing mole fraction of water in the solvent mixture. An extrapolation of the new data to pure water results in partial molar volumes of CO_2

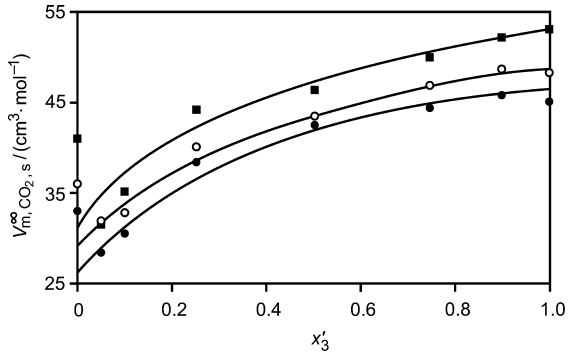

Figure 9. Influence of the mole fraction of DMF x'_3 in the gas-free solvent on the partial molar volume at infinite dilution in aqueous solutions of DMF: ■, $T \approx 314$ K; ○, $T \approx 354$ K; ●, $T \approx 395$ K. Data for $x'_3 = 0$ (i.e., for water) from the correlation by Brelvi and O'Connell.[80]

that lie about 10 cm^3·mol^{-1} below the prediction results from the method by Brelvi and O'Connell.

The influence of the solvent composition on the partial molar volume $V^{\infty}_{m,CO_2,s}$ was approximated by an equation similar to eq 11, but neglecting the influence of temperature on the Redlich–Kister parameters:

$$V^{\infty}_{m,CO_2,s} = V^{\infty}_{m,CO_2,W} + x'_3[V^{\infty}_{m,CO_2,DMF} - V^{\infty}_{m,CO_2,W}] + x'_2x'_3[A_{V,0} + (x'_3 - x'_2)A_{V,1} + (x'_3 - x'_2)^2A_{V,2}] \tag{15}$$

where $V^{\infty}_{m,CO_2,W}$ and $V^{\infty}_{m,CO_2,DMF}$ are the partial molar volumes of CO_2 at infinite dilution in water and DMF, respectively, and $A_{V,0}$, $A_{V,1}$, and $A_{V,2}$ are Redlich–Kister parameters. The Redlich–Kister parameters as well as the partial molar volume of CO_2 in pure water $V^{\infty}_{m,CO_2,W}$ were fit to the new experimental results; that is, the prediction results for $V^{\infty}_{m,CO_2,W}$ from the method of Brelvi and O'Connell were not considered for that correlation. The results from that fit are given in Table 7. The correlation reproduces the experimental results for $V^{\infty}_{m,CO_2,s}$ with a standard deviation of 1.1 cm^3·mol^{-1}. The maximum deviation is 2.4 cm^3·mol^{-1} at 354.4 K and $x'_3 = 0.9$.

COMPARISON WITH LITERATURE DATA FOR THE PARTIAL MOLAR VOLUME OF CO_2 IN DMF

Chang et al.[84] also measured the density (by vibrating tube densimetry) of liquid mixtures of (DMF and CO_2) at (291, 301, and 310) K. Their data were converted to allow an evaluation according to eq 14. As expected, also at those lower temperatures, the linear relation between $V/\tilde{m}_s$ and m_{CO_2} holds up to large gas molalities. The results for the partial molar volume of CO_2 in DMF at infinite dilution $V^{\infty}_{m,CO_2,DMF}$ are 43.4 cm^3·mol^{-1} (at 290.8 K), 41.3 cm^3·mol^{-1} (at 300.8 K), and 44.5 cm^3·mol^{-1} (at 310.1 K). The uncertainty resulting from the extrapolation procedure is estimated to ± 3 cm^3·mol^{-1}. The good agreement between the results from the data by Chang et al. for 310.1 K with the results of the present work at 313.8 K (45.1 cm^3·mol^{-1}) is another indication for the suspicion

dx.doi.org/10.1021/je300105q | J. Chem. Eng. Data 2012, 57, 1249–1266

mentioned above when the experimental results for the total pressure above (DMF + CO_2) were compared—as small amounts of a sparsely soluble gas are expected to have a very small influence on $V^{\infty}_{m,CO_2,DMF}$.

Kordikowski et al.[88] reported experimental results for the density of liquid mixtures of (DMF + CO_2) at (298.15, 303.15, and 313.15) K at pressures up to 7.6 MPa (reporting also the density of the pure solvent DMF). An evaluation of that experimental data according to eq 14 reveals only a minor influence of temperature on $V^{\infty}_{m,CO_2,DMF}$. The numerical values for $V^{\infty}_{m,CO_2,DMF}$ slightly depend on the evaluation procedure (number of data points used in the correlation, linear fit, or quadratic fit of $V/(\tilde{m}_{DMF})$ versus m_{CO_2}, etc.) and scatter between 37.6 $cm^3 \cdot mol^{-1}$ (at 298 K) and 40.0 $cm^3 \cdot mol^{-1}$ (at 313 K). They are always smaller than the numbers that were extrapolated from the results of the present work (43.3 $cm^3 \cdot mol^{-1}$ (at 298 K) and 44.8 $cm^3 \cdot mol^{-1}$ (at 313 K)). However, we assume that the differences are smaller than the sum of the experimental uncertainties of both investigations.

The most comprehensive study on the density of liquid mixtures of (CO_2 + DMF) was performed by Zúñiga-Moreno and Galicia-Luna[92] by vibrating tube densimetry at temperatures from (313 to 363) K and pressures between (3 and 25) MPa. Their density data were used to determine $V^{\infty}_{m,CO_2,DMF}$ at (313 and 353) K. In that evaluation it was assumed that in the range of composition and pressure that are of interest here the partial molar volumes of both components only depend on temperature (i.e., they depend neither on the composition of the liquid mixture nor on pressure). Thus, the following equation was applied to calculate $V^{\infty}_{m,CO_2,DMF}$:

$$x_{CO_2} \cdot V^{\infty}_{m,CO_2,DMF} + (1 - x_{CO_2}) \cdot \frac{M_{DMF}}{\rho_{DMF}} = \frac{x_{CO_2} \cdot M_{CO_2} + (1 - x_{CO_2}) \cdot M_{DMF}}{\rho_{mix}} \quad (16)$$

Each experimental data point for the density of a liquid mixture of (CO_2 + DMF), ρ_{mix}, from the publication by Zúñiga-Moreno and Galicia-Luna[92] (at mole fractions of CO_2 up to about 0.6 and pressures up to about 11 MPa) was used (together with their experimental results for the density of pure DMF, ρ_{DMF}) to calculate $V^{\infty}_{m,CO_2,DMF}$. The resulting average number for $V^{\infty}_{m,CO_2,DMF}$ is $(43.4^{+2.2}_{-1.6})$ $cm^3 \cdot mol^{-1}$ at 313 K and (47.5 ± 0.5) $cm^3 \cdot mol^{-1}$ at 353 K. These values agree excellently with the results of the present investigation (cf., Table 9) $V^{\infty}_{m,CO_2,DMF}$ = 45.1 $cm^3 \cdot mol^{-1}$ at 314 K and 48.3 $cm^3 \cdot mol^{-1}$ at 354 K.

CORRELATION OF VAPOR–LIQUID EQUILIBRIUM

The correlation of the new experimental data for the solubility of CO_2 in DMF and aqueous solutions of DMF combines the extended Henry's law on the molality scale for the solute, that is, carbon dioxide (component 1)

$$k^{m,0}_{H,CO_2,s} \exp\left[\frac{V^{\infty}_{CO_2,s} p}{RT}\right] a_{CO_2} = f^{V}_{CO_2} \quad (17)$$

with the extended Raoult's law for the solvent components

$$p^s_i \phi^s_i \exp\left[\frac{v_i(p - p^s_i)}{RT}\right] a_i = y_i p \phi_i \quad (i = 2(\text{water}), 3(\text{DMF})) \quad (18)$$

Two approaches were applied. In approach A the fugacity of carbon dioxide in the vapor phase was described by the virial equation that was truncated after the second virial coefficient:

$$f^{V}_{CO_2} = y_{CO_2} p \phi_{CO_2} \quad (19)$$

The details of that method are described above in the section on the evaluation of the experimental data to determine Henry's constant.

As the truncated virial equation is not a good approximation when the pressure is high and the temperature is low, also an approach B was applied. Here it was assumed that the amount of both solvent components in the vapor phase is so small that it can be neglected; that is, approach B assumes that the vapor consists of pure carbon dioxide. Then, the phase equilibrium description reduces to:

$$k^{m,0}_{H,CO_2,s} \exp\left[\frac{V^{\infty}_{CO_2,s} p}{RT}\right] a_{CO_2} = f^{V}_{CO_2,pure}(T, p) \quad (20)$$

The fugacity of pure carbon dioxide was calculated using the equation of state of Span and Wagner[72] via the *Thermofluids* software package.[79] That assumption is a good approximation at high pressures and low temperatures, but it does not allow to estimate the vapor phase mole fractions of the solvent components and certainly fails at low partial pressures of carbon dioxide.

The liquid phase was always (in approaches A and B) described with the method of Pérez-Salado Kamps[67] which is an extension of Pitzer's expression[85,86] for the excess Gibbs energy of aqueous electrolyte solutions to solvent mixtures. The activity of the solute component becomes:

$$a_{CO_2} = \frac{m_{CO_2}}{m^{\circ}} \gamma^*_{CO_2} \quad (21)$$

where $\gamma^*_{CO_2}$—the activity coefficient of CO_2 in the solvent mixture—is expressed using a binary (β_{CO_2,CO_2}) and a ternary parameter (μ_{CO_2,CO_2,CO_2}) for interactions between solute species in the solvent mixture:

$$\ln \gamma^*_{CO_2} = 2\frac{m_{CO_2}}{m^{\circ}} \beta_{CO_2,CO_2} + 3\left(\frac{m_{CO_2}}{m^{\circ}}\right)^2 \mu_{CO_2,CO_2,CO_2} \quad (22)$$

Both interaction parameters depend on temperature and solvent composition:

$$\beta_{CO_2,CO_2} = \beta_{CO_2,CO_2}(T, x'_3) \quad (23a)$$

$$\mu_{CO_2,CO_2,CO_2} = \mu_{CO_2,CO_2,CO_2}(T, x'_3) \quad (23b)$$

The activity of a solvent component follows from eq 4 that has to be extended to consider the contribution from the

dx.doi.org/10.1021/je300105q | J. Chem. Eng. Data 2012, 57, 1249–1266

interactions between the solutes and the particular selection of the reference state for the solute:

$$a_i = x_i\gamma_i(T, x'_3)\gamma_{i,\mathrm{conv}}(T, x'_3, m_1)\gamma_{i,\mathrm{Pitzer}}(T, x'_3, m_1)\gamma_{i,\mathrm{ref}}(T, x'_3, m_1) \qquad (i = 2, 3) \tag{24}$$

where x_i, $\gamma_i(T,x'_3)$, and $\gamma_{i,\mathrm{conv}}(T,x'_3,m_1)$ are given by eqs 5, 7b, and 8, respectively, and $\gamma_{i,\mathrm{Pitzer}}(T,x'_3,m_1)$ and $\gamma_{i,\mathrm{ref}}(T,x'_3,m_1)$ are (cf. refs 67 and 87), for $i = 2$ (i.e., for water):

$$\ln \gamma_{2,\mathrm{Pitzer}}(T, x'_3, m_1) = -M_2^*\left[\left(\frac{m_{\mathrm{CO_2}}}{m^\circ}\right)^2\beta_{\mathrm{CO_2,CO_2}} + 2\left(\frac{m_{\mathrm{CO_2}}}{m^\circ}\right)^3\mu_{\mathrm{CO_2,CO_2,CO_2}}\right] - M_s^*x'_3\left[\left(\frac{m_{\mathrm{CO_2}}}{m^\circ}\right)^2\frac{\partial\beta_{\mathrm{CO_2,CO_2}}}{\partial x'_3} + \left(\frac{m_{\mathrm{CO_2}}}{m^\circ}\right)^3\frac{\partial\mu_{\mathrm{CO_2,CO_2,CO_2}}}{\partial x'_3}\right] \tag{25a}$$

$$\ln \gamma_{2,\mathrm{ref}}(T, x'_3, m_1) = -x'_3M_s^*\left(\frac{m_{\mathrm{CO_2}}}{m^\circ}\right)\left[\left(\frac{\partial \ln\left(\frac{k^{\mathrm{m},0}_{\mathrm{H,CO_2,s}}(T,x'_3)}{k^{\mathrm{m},0}_{\mathrm{H,CO_2,W}}(T)}\right)}{\partial x'_3}\right)_T + \frac{p}{RT}\left(\frac{\partial V^{\infty}_{\mathrm{m,CO_2,s}}}{\partial x'_3}\right)_T - \frac{(M_3^* - M_2^*)}{M_s^*}\right] \tag{25b}$$

and for $i = 3$ (i.e., for DMF):

$$\ln \gamma_{3,\mathrm{Pitzer}}(T, x'_3, m_1) = -M_3^*\left[\left(\frac{m_{\mathrm{CO_2}}}{m^\circ}\right)^2\beta_{\mathrm{CO_2,CO_2}} + 2\left(\frac{m_{\mathrm{CO_2}}}{m^\circ}\right)^3\mu_{\mathrm{CO_2,CO_2,CO_2}}\right] + M_s^*(1 - x'_3)\left[\left(\frac{m_{\mathrm{CO_2}}}{m^\circ}\right)^2\frac{\partial\beta_{\mathrm{CO_2,CO_2}}}{\partial x'_3} + \left(\frac{m_{\mathrm{CO_2}}}{m^\circ}\right)^3\frac{\partial\mu_{\mathrm{CO_2,CO_2,CO_2}}}{\partial x'_3}\right] \tag{26a}$$

$$\ln \gamma_{3,\mathrm{ref}}(T, x'_3, m_1) = (1 - x'_3)M_s^*\left(\frac{m_{\mathrm{CO_2}}}{m^\circ}\right)\left[\left(\frac{\partial \ln\left(\frac{k^{\mathrm{m},0}_{\mathrm{H,CO_2,s}}(T,x'_3)}{k^{\mathrm{m},0}_{\mathrm{H,CO_2,W}}(T)}\right)}{\partial x'_3}\right)_T + \frac{p}{RT}\left(\frac{\partial V^{\infty}_{\mathrm{m,CO_2,s}}}{\partial x'_3}\right)_T - \frac{(M_3^* - M_2^*)}{M_s^*}\right] \tag{26b}$$

The calculations applied the experimental results for Henry's constants in the pure solvent and eq 11 to describe the influence of solvent composition on the Henry's constant (at zero pressure). The influence of pressure on Henry's constant is taken into account by eq 17. The influence of temperature and composition on the partial molar volume of CO_2 at infinite dilution in the solvents was described by eq 15.

In both correlation methods, the influence of temperature and solvent composition was approximated by a Redlich–Kister type of expression:

$$\beta_{\mathrm{CO_2,CO_2}}(T, x'_3) = x'_2\beta_{\mathrm{CO_2,CO_2}}(T, x'_3 = 0) + x'_3\beta_{\mathrm{CO_2,CO_2}}(T, x'_3 = 1) + x'_2x'_3[A_{\beta,0} + (x'_3 - x'_2)A_{\beta,1} + (x'_3 - x'_2)^2A_{\beta,2}] \tag{27}$$

and

$$\mu_{\mathrm{CO_2,CO_2,CO_2}}(T, x'_3) = x'_2\mu_{\mathrm{CO_2,CO_2,CO_2}}(T, x'_3 = 0) + x'_3\mu_{\mathrm{CO_2,CO_2,CO_2}}(T, x'_3 = 1) + x'_2x'_3[A_{\mu,0} + (x'_3 - x'_2)A_{\mu,1} + (x'_3 - x'_2)^2A_{\mu,2}] \tag{28}$$

where ($\beta_{\mathrm{CO_2,CO_2}}(T,x'_3 = 0)$ and $\beta_{\mathrm{CO_2,CO_2}}(T,x'_3 = 1)$) and ($\mu_{\mathrm{CO_2,CO_2,CO_2}}(T,x'_3 = 0)$ and $\mu_{\mathrm{CO_2,CO_2,CO_2}}(T,x'_3 = 1)$) are the binary and ternary parameters for interactions between CO_2 molecules in water (i.e, $x'_3 = 0$) and in DMF (i.e, $x'_3 = 1$). The parameters for interactions in water were set to zero.[6]

Results for Method A. The (temperature-dependent) parameters for interactions between CO_2 molecules in pure DMF were fit to all new experimental results for the solubility of CO_2 in DMF. A restriction to low gas molalities and low pressures (see below) showed no significant improvement. The results for $\beta_{\mathrm{CO_2,CO_2}}(T,x'_3 = 1)$ and $\mu_{\mathrm{CO_2,CO_2,CO_2}}(T,x'_3 = 1)$ are given in Table 12. The correlation results for the total pressure above (DMF + CO_2) agree with the experimental results with a standard deviation of 2.2 % at 314 K, 0.5 % at 354 K, and 1.0 % at 395 K. The maximum deviations amount to 5.3 % at 314 K (at $m_{\mathrm{CO_2}} = 0.261$ mol·kg^{-1} and $p = 0.141$ MPa), 1.2 % at 354 K (at $m_{\mathrm{CO_2}} = 2.4$ mol·kg^{-1} and $p = 2.37$ MPa), and 2.0 % at 395 K

dx.doi.org/10.1021/je300105q | J. Chem. Eng. Data 2012, 57, 1249–1266

Table 12. Correlation of the Gas Solubility Measurements by Method A

T/K	314.0	354.4	395.0
$\beta_{CO_2,CO_2}(T, x'_3 = 1)$	−0.03615	−0.04329	−0.04574
$\mu_{CO_2,CO_2,CO_2}(T, x'_3 = 1)$	0.000292	0.000522	0.000445
first modification	all temperatures (m_{CO_2} < 10 mol·kg^{-1}; p < 7 MPa)		
$A_{\beta,0}$	−0.22452		
$A_{\beta,1}$	0.20586		
$A_{\beta,2}$	0.043254		
$A_{\mu,0}$	0.0055806		
$A_{\mu,1}$	−0.0089273		
$A_{\mu,2}$	−0.0017068		
second modification	all temperatures, all experimental data points		
$A_{\beta,0}$	−0.20636		
$A_{\beta,1}$	0.19195		
$A_{\beta,2}$	0.015682		
$A_{\mu,0}$	0.0039984		
$A_{\mu,1}$	−0.0063330		
$A_{\mu,2}$	0.0015541		

(at m_{CO_2} = 1.93 mol·kg^{-1} and p = 3.03 MPa). The good agreement was not expected as on one side the virial equation is not a good choice at the higher pressures, and on the other side, the molality-scale-based model for the excess Gibbs energy of the liquid mixture cannot be expected to be a good choice at the very high gas molalities. For example, at m_{CO_2} = 30 mol·kg^{-1}, the dominating component in the liquid mixture is no longer DMF but CO_2 (mole fraction of CO_2 ≈ 0.7).

All remaining parameters (which describe the influence of composition on the binary and ternary interaction parameter between CO_2 molecules) are assumed to be independent of temperature. They were fit to the experimental results for the total pressure when CO_2 is dissolved in aqueous solutions of DMF. Two modifications of approach A were considered. In the first modification only those experimental data were considered where either the molality of carbon dioxide did not exceed 10 mol·kg^{-1} DMF and/or the pressure was below 7 MPa, whereas in the second modification all experimental data points were used to adjust the model parameters. The resulting parameter sets are shown in Table 12. The first modification represents the experimentally determined total pressures that were used for fitting the parameters with a standard deviation of 2.5 % and results in a standard deviation of 5.8 % over all experimental data points. The second modification gives a standard deviation of 3.6 % over all experimentally determined total pressures and of 2.5 % for the data points considered in the first modification. The small differences reveal that—as expected—the interaction parameters of the model for the liquid phase can also correct some failures of the method to describe the properties of the vapor phase. Figure 10 shows the influence of solvent composition and temperature on the binary and ternary interaction parameters from the second modification. Both parameters show an S-shape behavior, that is, with changing solvent composition both parameters run through a minimum as well as through a maximum.

The correlation presented here is aimed to describe gas solubility in terms of the total pressure versus the molality of the dissolved gas. Therefore, one may expect that the model correctly predicts the gas phase composition at low gas molalities, but not at high gas molalities (as no experimental data for the vapor phase composition was available). The

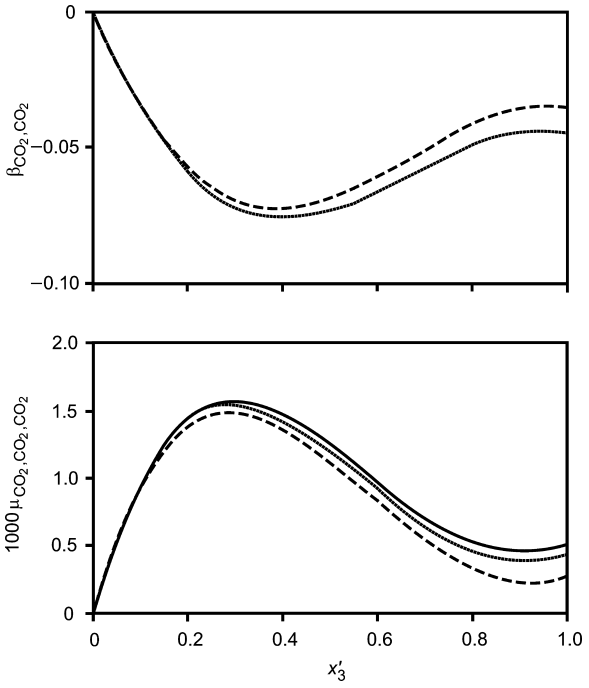

Figure 10. Influence of the mole fraction of DMF x'_3 in the gas-free solvent on the binary and ternary interaction parameters β_{CO_2,CO_2} and μ_{CO_2,CO_2,CO_2} (method A; parameters fit to all experimental data): broken line: T = 314 K; dotted line: T = 395 K; full line: T = 354 K.

capability of the model (with the current parameter set) to predict the gas-phase composition was tested by way of example. Prediction results for the composition of the vapor phase above liquid mixtures of (CO_2 + DMF) are compared with experimental results reported by Schlichting[83] who measured the vapor-phase composition by a dynamic gas saturation technique at (293, 313, and 338) K at pressures up to about 10 MPa. The experimental results showed—for all investigated temperatures—that the small vapor phase mole fraction of DMF runs through a minimum when the pressure is increased. As a typical example Figure 11 shows the results by

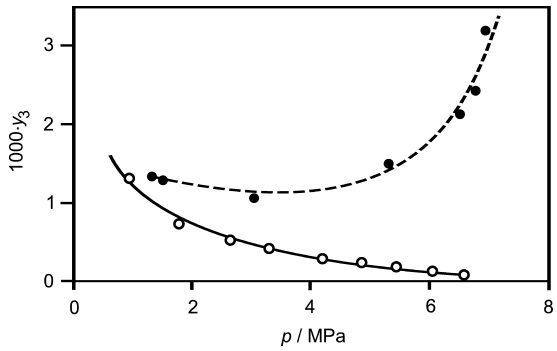

Figure 11. Vapor−liquid equilibrium of (CO_2 + DMF) at T = 313 K: Experimental results (Schlichting[83]) and prediction results (present work, second modification of model A) for the vapor-phase mole fraction of DMF y_3: ●, experimental data; ○, prediction results.

Schlichting in comparison with predictions from the correlation. The prediction results for the vapor-phase mole fraction of DMF steadily decrease with increasing pressure. Only at low pressures the prediction results agree reasonably with the experimental data. However, at high pressures (i.e., at

dx.doi.org/10.1021/je300105q | J. Chem. Eng. Data 2012, 57, 1249−1266

gas molalities, where DMF is no longer the main component of the liquid phase) the prediction results deviate systematically from the experimental data. Schlichting[83] discussed the uncertainties of his experiments. The largest uncertainty (estimated to 50 %) might be caused by an incomplete saturation of CO_2 in the liquid phase. However, at high pressures the deviations between Schlichting's experimental results and the predictions for the vapor-phase mole fraction of CO_2 reach some orders of magnitude. This is a hint that—as already mentioned above—the shortcomings of the model (Pitzer's molality-scale-based G^E-model with DMF as the background solvent but DMF being no longer the main component in the liquid phase + truncated virial equation) are compensated by the flexibility of the model resulting in parameters for interactions in the liquid phase that have only a limited physical meaning.

Results for Method B. Method B assumes that the vapor phase is pure carbon dioxide. Therefore, that model should only be used when the mole fraction of CO_2 in the vapor phase is sufficiently large (here: $y_{CO_2} > 0.98$ (at (314 and 354) K) and $y_{CO_2} > 0.9$ (at 395 K)). The vapor phase mole fraction was estimated from the vapor pressure p_s^{sat} above the binary, gas-free solvent mixture (water + DMF) and the total pressure p that is required to dissolve CO_2 in that solvent mixture:

$$y_{CO_2,estim} = (p - p_s^{sat})/p \quad (29)$$

As in method A, the binary and ternary parameters for interactions between dissolved carbon dioxide were considered to depend on temperature and solvent composition. The experimental results for the solubility of CO_2 in DMF were used to fit $\beta_{CO_2,CO_2}(T, x'_3 = 1)$ and $\mu_{CO_2,CO_2,CO_2}(T, x'_3 = 1)$ as to minimize the deviation between the correlation results and the experimental results for the molality of CO_2 in the liquid phase. As in method A, the calculations were based on the experimental results for the Henry's constants in the pure solvents and on eq 11 to describe the influence of solvent composition on the Henry's constant. The influence of pressure on Henry's constant was described by eq 20. The influence of temperature and composition on the partial molar volume of CO_2 at infinite dilution in the solvents was described by eq 15. The set of parameters is given in Table 13. The correlation results agree with the experimentally determined molalities of CO_2 in pure DMF (at 314 K and $y_{CO_2,estim} > 0.98$), (at 354 K and $y_{CO_2,estim} > 0.98$), and (at 395 K and $y_{CO_2,estim} > 0.9$) with a standard deviation of 1.9 %, 0.5 %, and 1.7 %, respectively. The experimental results for the solubility of CO_2 in aqueous solutions of DMF were then used to determine the influence of solvent composition on the binary and ternary interaction parameters. That influence was described by eqs 27 and 28 assuming that the Redlich–Kister parameters do not depend on temperature. The fitting procedure followed the outline given above. The Redlich–Kister parameters $A_{\beta,i}$ and $A_{\mu,i}$ (for i = 0, 1, and 2) are given in Table 13. The influence of solvent composition and temperature on the binary and ternary interaction parameters resembles the behavior already shown in Figure 10. Both parameters show an S-shape behavior, that is, with increasing mole fraction of DMF both parameters run through a minimum as well as through a maximum. The correlation represents the experimentally determined molalities of CO_2 in aqueous solutions of DMF (for $y_{CO_2,estim} > 0.98$ (at (314 and 354) K) and $y_{CO_2,estim} > 0.9$ at 395 K) with a standard deviation of 3.47 %. Reducing the database to lower gas molalities does not result in an improvement. For example, the standard deviation (for the considered data set) slightly increases from 3.47 % to 3.55 % (3.63 %) when the maximum gas molality is limited to $m_{CO_2} < 10$ mol·kg^{-1} ($m_{CO_2} < 5$ mol·kg^{-1}). As expected the interaction parameters from all three correlations (first and second modification of method A and method B) attain similar numerical values, but one should keep in mind that small changes in those parameters can have an important influence on the calculated data (total pressures and molalities of dissolved CO_2, respectively). Finally it should be mentioned that both the activity coefficient of CO_2 and the Krichevsky–Kasarnovsky factor that describes the influence of pressure on Henry's constant (cf. eqs 17 and 20–22) have an important influence on the calculation results. For example, for the solubility of CO_2 in pure DMF at T = 314 K and p = 6.6 MPa (i.e., at the highest investigated gas molality m_{CO_2} = 31 mol·kg^{-1}) the Krichevsky–Kasarnovsky factor becomes $\exp[V^{\infty}_{CO_2,s}p/(RT)] = 1.12$ and the correlation method B gives for the activity coefficient of carbon dioxide $\gamma^*_{CO_2} = 0.227$.

Table 13. Correlation of the Gas Solubility Measurements by Method B

T/K	314.0	354.4	395.0
$\beta_{CO_2,CO_2}(T, x'_3 = 1)$	−0.03731	−0.04370	−0.04546
$\mu_{CO_2,CO_2,CO_2}(T, x'_3 = 1)$	0.000289	0.000454	0.000369
	at 314 and 354 K: $y_{CO_2} > 0.98$; at 395 K: $y_{CO_2} > 0.90$		
$A_{\beta,0}$	−0.189234		
$A_{\beta,1}$	0.213595		
$A_{\beta,2}$	−0.108086		
$A_{\mu,0}$	0.0015951		
$A_{\mu,1}$	−0.0012252		
$A_{\mu,2}$	−0.00078686		

Both correlation methods were also used to compare calculation results for the solubility of CO_2 in DMF at (294 and 338) K with the experimental results of Duran-Valencia et al.[89] For (294 and 338) K, the interaction parameters $\beta_{CO_2,CO_2}(T, x'_3 = 1)$ and $\mu_{CO_2,CO_2,CO_2}(T, x'_3 = 1)$ required for these calculations were extrapolated (for 294 K) or interpolated (for 338 K) from the results given in Tables 12 and 13, respectively. The comparison was restricted to $m_{CO_2} < 16$ (mol·kg^{-1}). The solubility pressure was calculated (using method A) for given temperature and liquid phase composition, whereas the molality of dissolved CO_2 was calculated (using method B) for given temperature and solubility pressure. For 294 K, the calculation results systematically deviate from the experimental results by Duran-Valencia et al.[89] The calculated results for the total pressure (molality of CO_2) are lower (higher) than the experimental data. The deviations between the experimental results and the calculation results from both methods reveal the same order of magnitude. The relative deviations decrease with increasing molality of CO_2 from about 10 % at $m_{CO_2} \leq 5$ (mol·kg^{-1}) to about 1 % at $m_{CO_2} \approx 15$ (mol·kg^{-1}). There is also a systematic deviation between the calculation results and the experimental data by Duran-Valencia et al. for 338 K. The calculated results for the total pressure (molality of CO_2) are higher (lower) than the experimental data. The relative deviation increases with increasing molality of CO_2 from about 2 % at $m_{CO_2} \leq 5$ (mol·kg^{-1}) to about 7 % at $m_{CO_2} \approx 16$ (mol·kg^{-1}).

CONCLUSIONS

Gas solubility in mixed solvent systems is an area of fluid phase equilibrium thermodynamics that has many applications in industry. Despite its importance, the amount of open accessible and reliable experimental data as well as the number of tested models for the correlation and prediction of such data is far from adequate. The present publication is aiming to contributing to that area. In an extension of previous investigations on the solubility of a single gas in organic solvents, aqueous solutions of organic solvents (without as well as with a strong electrolyte) the solubility of carbon dioxide in pure liquid *N*,*N*-dimethylmethanamide (commonly known as dimethylformamide or DMF) and in aqueous solutions of DMF at temperatures from about 314 K to about 395 K and pressures up to about 10 MPa was determined experimentally with a synthetic technique. The mole fraction of DMF in the aqueous, gas-free solutions was varied between 0.05 and 1. The Henry's constant of carbon dioxide in pure liquid DMF as well as in the solvent mixtures was evaluated from those new experimental results. The volumetric data that were measured in the gas solubility measurements were used to determine the partial molar volume of CO_2 in those solutions. Such data are in particular important to estimate the volume expansion of liquids caused by well soluble gases. The vapor−liquid equilibrium data were correlated by applying an extension of Pitzer's model for aqueous electrolyte solutions to describe the gas solubility in mixed solvents. The results for the binary system (DMF + CO_2) were compared to the rather limited experimental information on that system that is available in the open literature. In ongoing research the investigations will be extended to the influence of a strong electrolyte on the solubility of CO_2 in (water + DMF).

AUTHOR INFORMATION

Corresponding Author

*Tel.: +49 631 205 2410. Fax: +49 631 205 3835. E-mail: gerd.maurer@mv.uni-kl.de.

Funding

Some parts of this work were supported by the German Government (BMBF Grant-No. 01/RK9808/8) and cosponsored by Siemens-Axiva GmbH & Co. KG, Lurgi Energie und Entsorgung GmbH, Lurgi Oel Gas Chemie GmbH, Degussa AG, Bayer AG, and BASF AG. Funding and cooperation is gratefully acknowledged.

Notes

The authors declare no competing financial interest.

REFERENCES

(1) Müller, G.; Bender, E.; Maurer, G. Das Dampf-Flüssigkeits-Gleichgewicht des ternären Systems Ammoniak-Kohlendioxid-Wasser bei hohen Wassergehalten im Bereich zwischen 373 und 473 K. *Ber. Bunsenges. Phys. Chem.* **1988**, *92*, 148−160.

(2) Göppert, U.; Maurer, G. Vapor-liquid equilibria in aqueous solutions of ammonia and carbon dioxide at temperatures between 333 and 393 K and pressures up to 7 MPa. *Fluid Phase Equilib.* **1988**, *41*, 153−185.

(3) Kling, G.; Maurer, G. The solubility of hydrogen in water and 2-aminoethanol at temperatures between 323 and 423 K and pressures up to 16 MPa. *J. Chem. Thermodyn.* **1991**, *23*, 531−541.

(4) Kling, G.; Maurer, G. Solubility of hydrogen in aqueous monoethanolamine solutions at temperatures between 323 and 423 K. *J. Chem. Eng. Data* **1991**, *36*, 390−394.

(5) Rumpf, B.; Maurer, G. Solubilities of hydrogen cyanide and sulfur dioxide in water at temperatures from 293.15 to 413.15 K and pressures up to 2.5 MPa. *Fluid Phase Equilib.* **1992**, *81*, 241−260.

(6) Rumpf, B.; Maurer, G. An experimental and theoretical investigation on the solubility of carbon dioxide in aqueous solutions of strong electrolytes. *Ber. Bunsenges. Phys. Chem.* **1993**, *97*, 85−97.

(7) Rumpf, B.; Weyrich, F.; Maurer, G. Simultaneous solubility of ammonia and sulfur dioxide in water at temperatures from 313.15 to 373.15 K and pressures up to 2.2 MPa. *Fluid Phase Equilib.* **1993**, *83*, 253−260.

(8) Rumpf, B.; Maurer, G. Solubility of ammonia in aqueous solutions of sodium- and ammonium sulfate at temperatures from 333.15 to 433.15 K and pressures up to 3 MPa. *Ind. Eng. Chem. Res.* **1993**, *32*, 1780−1789.

(9) Rumpf, B.; Maurer, G. Solubility of sulfur dioxide in aqueous solutions of sodium- and ammonium sulfate at temperatures from 313.15 to 393.15 K and pressures up to 3.5 MPa. *Fluid Phase Equilib.* **1993**, *91*, 113−131.

(10) Rumpf, B.; Maurer, G. Solubility of ammonia in aqueous solutions of phosphoric acid: Model development and application. *J. Solution Chem.* **1994**, *23*, 37−51.

(11) Rumpf, B.; Nicolaisen, H.; Öcal, C.; Maurer, G. Solubility of carbon dioxide in aqueous solutions of sodium chloride: Experimental results and modeling. *J. Solution Chem.* **1994**, *23*, 431−448.

(12) Rumpf, B.; Nicolaisen, H.; Maurer, G. Solubility of carbon dioxide in aqueous solutions of ammonium chloride at temperatures from 313 to 433 K and pressures up to 10 MPa. *Ber. Bunsenges. Phys. Chem.* **1994**, *98*, 1077−1081.

(13) Kurz, F.; Rumpf, B.; Maurer, G. Vapor-liquid-solid phase equilibria in the system NH_3-CO_2-H_2O from around 310 to 470 K: New experimental data and modeling. *Fluid Phase Equilib.* **1995**, *104*, 261−275.

(14) Bieling, V.; Kurz, F.; Rumpf, B.; Maurer, G. Simultaneous solubility of ammonia and carbon dioxide in aqueous solutions of sodium sulfate in the temperature range from 313 to 393 K and pressures up to 3 MPa. *Ind. Eng. Chem. Res.* **1995**, *34*, 1449−1460.

(15) Kuranov, G.; Rumpf, B.; Smirnova, N. A.; Maurer, G. Solubility of single gases carbon dioxide and hydrogen sulfide in aqueous solutions of N-methyldiethanolamine in the temperature range from 313 to 413 K and pressures up to 10 MPa. *Ind. Eng. Chem. Res.* **1996**, *35*, 1959−1966.

(16) Kurz, F.; Rumpf, B.; Maurer, G. Simultaneous solubility of ammonia and carbon dioxide in aqueous solutions of ammonium sulfate + sodium sulfate at temperatures from 313 to 393 K and pressures up to 10 MPa. *J. Chem. Thermodyn.* **1996**, *28*, 497−520.

(17) Kurz, F.; Rumpf, B.; Sing, R.; Maurer, G. Vapor-liquid and vapor-liquid-solid equilibria in the system ammonia−carbon dioxide−sodium chloride−water at temperatures from 313 to 393 K and pressures up to 3 MPa. *Ind. Eng. Chem. Res.* **1996**, *35*, 3795−3802.

(18) Rumpf, B.; Xia, J.; Maurer, G. An experimental investigation on the solubility of carbon dioxide in aqueous solutions containing sodium nitrate or ammonium nitrate at temperatures from 313 to 433 K and pressures up to 10 MPa. *J. Chem. Thermodyn.* **1997**, *29*, 1101−1111.

(19) Rumpf, B.; Xia, J.; Maurer, G. Solubility of carbon dioxide in aqueous solutions containing acetic acid or sodium hydroxide in the temperature range from 313 to 433 K and total pressures up to 10 MPa. *Ind. Eng. Chem. Res.* **1998**, *37*, 2012−2019.

(20) Xia, J.; Rumpf, B.; Maurer, G. Solubility of carbon dioxide in aqueous solutions containing sodium acetate or ammonium acetate at temperatures from 313 to 433 K at pressures up to 10 MPa. *Fluid Phase Equilib.* **1999**, *155*, 107−125.

(21) Rumpf, B.; Pérez-Salado Kamps, Á.; Sing, R.; Maurer, G. Simultaneous solubility ammonia and hydrogen sulfide in water at temperatures from 313 to 393 K. *Fluid Phase Equilib.* **1999**, *158−160*, 923−932.

(22) Xia, J.; Rumpf, B.; Maurer, G. The solubility of sulfur dioxide in aqueous solutions of acetic acid, sodium acetate and ammonium acetate in the temperature range from 313 to 393 K at pressures up to

3.3 MPa: Experimental results and comparison with correlations/predictions. *Ind. Eng. Chem. Res.* **1999**, *38*, 1149−1158.
(23) Sing, R.; Rumpf, B.; Maurer, G. Solubility of hydrogen sulfide in aqueous solutions of single strong electrolytes sodium nitrate, ammonium nitrate, and sodium hydroxide. *Ind. Eng. Chem. Res.* **1999**, *38*, 2098−2109.
(24) Xia, J.; Rumpf, B.; Maurer, G. The solubility of sulfur dioxide in aqueous solutions of sodium chloride and ammonium chloride in the temperature range from 313 to 393 K at pressures up to 3.7 MPa: Experimental results and comparison with correlations/predictions. *Fluid Phase Equilib.* **1999**, *165*, 99−119.
(25) Xia, J.; Pérez-Salado Kamps, Á.; Rumpf, B.; Maurer, G. The solubility of hydrogen sulfide in aqueous solutions of single salts sodium sulfate, ammonium sulfate, sodium chloride and ammonium chloride in the temperature range from 313 to 393 K and total pressures up to 10 MPa. *Ind. Eng. Chem. Res.* **2000**, *39*, 1064−1073.
(26) Xia, J.; Pérez-Salado Kamps, Á.; Rumpf, B.; Maurer, G. Solubility of hydrogen sulfide in aqueous solutions of single strong electrolytes sodium nitrate, ammonium nitrate, and sodium hydroxide at temperatures from 313 to 393 K and total pressures up to 10 MPa. *Fluid Phase Equilib.* **2000**, *167*, 263−284.
(27) Xia, J.; Pérez-Salado Kamps, Á.; Rumpf, B.; Maurer, G. Solubility of H_2S in (H_2O + CH_3COONa) and (H_2O + CH_3COONH_4) from 313 to 393 K and pressures up to 10 MPa. *J. Chem. Eng. Data* **2000**, *45*, 194−201.
(28) Pérez-Salado Kamps, Á.; Sing, R.; Rumpf, B.; Maurer, G. Influence of NH_4Cl, NH_4NO_3 and $NaNO_3$ on the simultaneous solubility of ammonia and carbon dioxide in water. *J. Chem. Eng. Data* **2000**, *45*, 796−809.
(29) Pérez-Salado Kamps, Á.; Balaban, A.; Jödecke, M.; Kuranov, G.; Smirnova, N. A.; Maurer, G. Solubility of single gases carbon dioxide and hydrogen sulfide in aqueous solutions of N-methydiethanolamine at temperatures from 313 to 413 K and pressures up to 7.6 MPa: new experimental data and model extension. *Ind. Eng. Chem. Res.* **2001**, *40*, 696−706.
(30) Anufrikov, Y.; Pérez-Salado Kamps, Á.; Kuranov, G.; Rumpf, B.; Smirnova, N. A.; Maurer, G. Solubility of CO_2 in H_2O + N-methydiethanolamine +(H_2SO_4 or Na_2SO_4). *AIChE J.* **2002**, *48*, 168−177.
(31) Anufrikov, Y.; Pérez-Salado Kamps, Á.; Kuranov, G.; Rumpf, B.; Smirnova, N. A.; Maurer, G. Solubility of H_2S in aqueous solutions of N-methydiethanolamine + (H_2SO_4 or Na_2SO_4). *Ind. Eng. Chem. Res.* **2002**, *41*, 2571−2578.
(32) Xia, J.; Pérez-Salado Kamps, Á.; Maurer, G. Solubility of H_2S in (H_2O + piperazine) and in (H_2O + MDEA + piperazine). *Fluid Phase Equilib.* **2003**, *207*, 23−34.
(33) Pérez-Salado Kamps, Á.; Xia, J.; Maurer, G. Solubility of CO_2 in (H_2O + piperazine) and in (H_2O + MDEA + piperazine). *AIChE J.* **2003**, *49*, 2662−2670.
(34) Pérez-Salado Kamps, Á.; Tuma, D.; Xia, J.; Maurer, G. Solubility of CO_2 in the ionic liquid [bmim][PF_6]. *J. Chem. Eng. Data* **2003**, *48*, 746−749.
(35) Xia, J.; Jödecke, M.; Pérez-Salado Kamps, Á.; Maurer, G. Solubility of CO_2 in (CH_3OH + H_2O). *J. Chem. Eng. Data* **2004**, *49*, 1756−1759.
(36) Kumełan, J.; Pérez-Salado Kamps, Á.; Tuma, D.; Maurer, G. Solubility of CO in in the ionic liquid [bmim][PF_6]. *Fluid Phase Equilib.* **2005**, *228−229*, 207−211.
(37) Kumełan, J.; Pérez-Salado Kamps, Á.; Urukova, I.; Tuma, D.; Maurer, G. Solubility of oxygen in the ionic liquid [bmim][PF_6]: Experimental and molecular simulation results. *J. Chem. Thermodyn.* **2005**, *37*, 595−602; **2007**, *39*, 335.
(38) Kumełan, J.; Pérez-Salado Kamps, Á.; Tuma, D.; Maurer, G. Solubility of H_2 in the ionic liquid [bmim][PF_6]. *J. Chem. Eng. Data* **2006**, *51*, 11−14.
(39) Pérez-Salado Kamps, Á.; Jödecke, M.; Xia, J.; Vogt, M.; Maurer, G. Influence of salts on the solubility of carbon dioxide in (water + methanol). Part I: sodium chloride. *Ind. Eng. Chem. Res.* **2006**, *45*, 1505−1515.
(40) Pérez-Salado Kamps, Á.; Jödecke, M.; Vogt, M.; Xia, J.; Maurer, G. Influence of salts on the solubility of carbon dioxide in (water + methanol). Part II: sodium sulfate. *Ind. Eng. Chem. Res.* **2006**, *45*, 3673−3677.
(41) Kumełan, J.; Pérez-Salado Kamps, Á.; Tuma, D.; Maurer, G. Solubility of CO_2 in the ionic liquid [hmim][Tf_2N]. *J. Chem. Thermodyn.* **2006**, *38*, 1396−1401.
(42) Kumełan, J.; Pérez-Salado Kamps, Á.; Tuma, D.; Maurer, G. Solubility of H_2 in the ionic liquid [hmim][Tf_2N]. *J. Chem. Eng. Data* **2006**, *51*, 1364−1367.
(43) Meyer, E.; Ermatchkov, V.; Pérez-Salado Kamps, Á.; Maurer, G. Simultaneous solubility of SO_2 and NH_3 in (salt + H_2O) and enthalpy change upon dilution of (SO_2 + NH_3 + salt + H_2O) in (salt + H_2O) {salt = $(NH_4)_2SO_4$ or Na_2SO_4}: Experimental results and model predictions. *Fluid Phase Equilib.* **2006**, *244*, 137−152.
(44) Ermatchkov, V.; Pérez-Salado Kamps, Á.; Maurer, G. Solubility of carbon dioxide in aqueous solutions of N-methyldiethanolamine in the low gas loading region. *Ind. Eng. Chem. Res.* **2006**, *45*, 6081−6091.
(45) Ermatchkov, V.; Pérez-Salado Kamps, Á.; Speyer, D.; Maurer, G. Solubility of carbon dioxide in aqueous solutions of piperazine in the low gas loading region. *J. Chem. Eng. Data* **2006**, *51*, 1788−1796.
(46) Kumełan, J.; Pérez-Salado Kamps, Á.; Tuma, D.; Maurer, G. Solubility of CO_2 in the ionic liquids [bmim][CH_3SO_4] and [bmim][PF_6]. *J. Chem. Eng. Data* **2006**, *51*, 1802−1807.
(47) Kumełan, J.; Pérez-Salado Kamps, Á.; Tuma, D.; Maurer, G. Solubility of the single gases H_2 and CO in the ionic liquid [bmim][CH_3SO_4]. *Fluid Phase Equilib.* **2007**, *260*, 3−8.
(48) Pérez-Salado Kamps, Á.; Meyer, E.; Rumpf, B.; Maurer, G. Solubility of CO_2 in aqueous solutions of KCl and in aqueous solutions of K_2CO_3. *J. Chem. Eng. Data* **2007**, *52*, 917−932.
(49) Jödecke, M.; Pérez-Salado Kamps, Á.; Maurer, G. Experimental investigation of the solubility of CO_2 in (acetone + water). *J. Chem. Eng. Data* **2007**, *52*, 1003−1009.
(50) Schäfer, D.; Xia, J.; Vogt, M.; Pérez-Salado Kamps, Á.; Maurer, G. Experimental investigation on the solubility of ammonia in methanol. *J. Chem. Eng. Data* **2007**, *52*, 1653−1659.
(51) Schäfer, D.; Vogt, M.; Pérez-Salado Kamps, Á.; Maurer, G. Solubility of ammonia in liquid mixtures of (water + methanol). *Fluid Phase Equilib.* **2007**, *261*, 306−312.
(52) Kumełan, J.; Pérez-Salado Kamps, Á.; Tuma, D.; Maurer, G. Solubility of the single gases methane and xenon in the ionic liquid [bmim][CH_3SO_4]. *J. Chem. Eng. Data* **2007**, *52*, 2319−2324.
(53) Kumełan, J.; Pérez-Salado Kamps, Á.; Tuma, D.; Maurer, G. Solubility of the single gases methane and xenon in the ionic liquid [hmim][Tf_2N]. *Ind. Eng. Chem. Res.* **2007**, *46*, 8236−8240.
(54) Kumełan, J.; Yokozeki, A.; Pérez-Salado Kamps, Á.; Shiflett, M. B.; Tuma, D.; Maurer, G. Solubility of CF_4 in the ionic liquid [hmim][Tf_2N]. *J. Phys. Chem. B* **2008**, *112*, 3040−3047.
(55) Schäfer, D.; Vogt, M.; Pérez-Salado Kamps, Á.; Maurer, G. Influence of a single salt ($NaCl/Na_2SO_4$) on the solubility of ammonia in liquid mixtures of (water + methanol). *Ind. Eng. Chem. Res.* **2008**, *47*, 5112−5118.
(56) Kumełan, J.; Tuma, D.; Verevkin, S. P.; Maurer, G. The solubility of hydrogen in the cyclic alkene ester 1,2-butylene carbonate. *J. Chem. Eng. Data* **2008**, *53*, 2844−2850.
(57) Kumełan, J.; Pérez-Salado Kamps, Á.; Tuma, D.; Maurer, G. Solubility of the single gases carbon monoxide and oxygen in the ionic liquid [hmim][Tf_2N]. *J. Chem. Eng. Data* **2009**, *54*, 966−971.
(58) Böttger, A.; Ermatchkov, V.; Maurer, G. Solubility of carbon dioxide in aqueous solutions of N-methyldiethanolamine and piperazine in the high gas loading region. *J. Chem. Eng. Data* **2009**, *54*, 1905−1909.
(59) Kumełan, J.; Pérez-Salado Kamps, Á.; Tuma, D.; Maurer, G. Solubility of the single gases carbon dioxide and hydrogen in the ionic liquid [bmpy][Tf_2N]. *J. Chem. Eng. Data* **2010**, *55*, 165−172.
(60) Speyer, D.; Ermatchkov, V.; Maurer, G. Solubility of carbon dioxide in aqueous solutions of N-methyldiethanolamine and piperazine in the low gas loading region. *J. Chem. Eng. Data* **2010**, *55*, 283−290.

(61) Speyer, D.; Maurer, G. Solubility of hydrogen sulfide dioxide in aqueous solutions of piperazine in the low gas loading region. *J. Chem. Eng. Data* **2011**, *56*, 763−767.
(62) Kumełan, J.; Pérez-Salado Kamps, Á.; Maurer, G. Solubility of CO_2 in aqueous solutions of methionine and in aqueous solutions of (K_2CO_3 + methionine). *Ind. Eng. Chem. Res.* **2010**, *49*, 3910−3918.
(63) Ermatchkov, V.; Maurer, G. Solubility of carbon dioxide in aqueous solutions of N-methyldiethanolamine and piperazine: Prediction and correlation. *Fluid Phase Equilib.* **2011**, *302*, 338−346.
(64) Schäfer, D.; Pérez-Salado Kamps, Á.; Maurer, G. Experimental investigation of the simultaneous solubility of chemical reactive gases NH_3 and CO_2 in liquid mixtures of (H_2O + CH_3OH) in liquid mixtures of (water + methanol). *J. Chem. Eng. Data* **2011**, *56*, 1084−1095.
(65) Kumełan, J.; Tuma, D.; Maurer, G. Simultaneous solubility of carbon dioxide and hydrogen in the ionic liquid [hmim][Tf_2N]: Experimental results and correlation. *Fluid Phase Equilib.* **2011**, *311*, 9−16.
(66) Kumełan, J.; Pérez-Salado Kamps, Á.; Tuma, D.; Maurer, G. Solubility of carbon dioxide in liquid mixtures of (water + [bmim][CH_3SO_4]. *J. Chem. Eng. Data* **2011**, *56*, 4505−4515.
(67) Pérez-Salado Kamps, Á. Model for the Gibbs Excess Energy of Mixed-Solvent (Chemical-Reacting and Gas-Containing) Electrolyte Systems. *Ind. Eng. Chem. Res.* **2005**, *44*, 201−225.
(68) Pérez-Salado Kamps, Á.; Vogt, M.; Jödecke, M.; Maurer, G. Investigation of the (solid-liquid and vapor-liquid) equilibrium of the system H_2O + CH_3OH + Na_2SO_4. *Ind. Eng. Chem. Res.* **2006**, *45*, 454−466.
(69) Jödecke, M.; Pérez-Salado Kamps, Á.; Maurer, G. Experimental investigation of the influence of NaCl on the vapor-liquid equilibrium of (CH_3OH + H_2O). *J. Chem. Eng. Data* **2005**, *50*, 138−141.
(70) Rumpf, B. Untersuchungen zur Löslichkeit reagierender Gase in Wasser und salzhaltigen wässrigen Lösungen. Ph.D. Dissertation, University of Kaiserslautern, Germany, 1992.
(71) Clever, H. L.; Battino, R. Solubility of Gases in Liquids. *The Experimental Determination of Solubilities; Wiley Series in Solution Chemistry*, Vol. *6*; Hefter, G. T., Tomkins, R. P. T., Eds.; John Wiley & Sons Ltd.: Chichester, England, 2003; pp 101−150.
(72) Span, R.; Wagner, W. A New Equation of State for Carbon Dioxide Covering the Fluid Region from the Triple-Point Temperature to 1100 K at Pressures up to 800 MPa. *J. Phys. Chem. Ref. Data* **1996**, *25*, 1509−1596.
(73) Saul, A.; Wagner, W. International equations for the saturation properties of ordinary water substance. *J. Phys. Chem. Ref. Data* **1987**, *16*, 893−901.
(74) *Detherm Datenbank*; Dechema: Frankfurt a.M. Germany, 2002.
(75) Dymond, J. H.; Smith, E. B. *The virial coefficients of pure gases and mixtures*; Oxford University Press: Oxford, U.K., 1980.
(76) Hayden, J. G.; O'Connell, J. P. A generalized method for predicting second virial coefficients. *Ind. Eng. Chem. Process. Des. Dev.* **1975**, *14*, 209−216.
(77) Bondi, A. *Physical Properties of Molecular Crystals, Liquids, and Glasses*; John Wiley & Sons: New York, 1968.
(78) Jödecke, M. Experimentelle und theoretische Untersuchungen zur Löslichkeit von Kohlendioxid in wässrigen, salzhaltigen Lösungen mit organischen Komponenten. Doctoral Dissertation, University of Kaiserslautern, Germany, 2004.
(79) Wagner, W. *Thermofluids*, Version 1.0, Build 1.0.0; Springer: Berlin, 2006.
(80) Brelvi, S. W.; O'Connell, J. P. Corresponding states correlations for liquid compressibility and partial molal volumes of gases at infinite dilution in liquids. *AIChE J.* **1972**, *18*, 1239−1243.
(81) Kumełan, J.; Tuma, D.; Maurer, G. Partial Molar Volumes of Selected Gases in Some Ionic Liquids. *Fluid Phase Equilib.* **2009**, *275*, 132−144.
(82) Melzer, W. M.; Schrödter, F.; Knapp, H. Solubilities of Methane, Propane and Carbon Dioxide in Solvent Mixtures Consisting of Water, *N,N*-Dimethylformamide, and N-methyl-2-Pyrrolidone. *Fluid Phase Equilib.* **1989**, *49*, 167−186.
(83) Schlichting, H. *Experimentelle Bestimmung und Korrelierung der Löslichkeit verschiedener Lösungsmittel in Hochdruckgasen*; Fortschr.-Ber. VDI, Reihe 3 Nr. 253, VDI-Verlag: Düsseldorf, Germany, 1991.
(84) Chang, C. J.; Chen, C.-Y.; Lin, H.-C. Solubilities of Carbon Dioxide and Nitrous Oxide in Cylohexanone, Toluene and *N,N*-Dimethylformamide at Elevated Pressures. *J. Chem. Eng. Data* **1995**, *40*, 850−855.
(85) Pitzer, K. S. Thermodynamics of Electrolytes. 1. Theoretical basis and general equations. *J. Phys. Chem.* **1973**, *77*, 268−277.
(86) Pitzer, K. S. Ion Interaction Approach: Theory and Data Correlation. In *Activity Coefficients in Electrolyte Solutions*; Pitzer, K. S., Ed.; CRC Press: Boca Raton, FL, 1991; pp 75−155.
(87) Urukova, I.; Pérez-Salado Kamps, Á.; Maurer, G. Solubility of CO_2 in (Water + Acetone): Correlation of experimental data and predictions from molecular simulation. *Ind. Eng. Chem. Res.* **2009**, *48*, 4553−4564.
(88) Kordikowski, A.; Schenk, A. P.; Van Nielen, R. M.; Peters, C. J. Volume expansions and vapor-liquid equilibria of binary mixtures of a variety of polar solvents and certain near-critical solvents. *J. Supercrit. Fluids* **1995**, *8*, 205−216.
(89) Duran-Valencia, C.; Valtz, A.; Galicia-Luna, L. A.; Richon, D. Isothermal vapour-liquid equilibria of the carbon dioxide (CO_2) - *N,N*-dimethylformamide (DMF) system at temperatures from 293.95 to 338.05 K and pressures up to 12 MPa. *J. Chem. Eng. Data* **2001**, *46*, 1589−1592.
(90) Byun, H.-S.; Kim, N.-H.; Kwak, C. Measurements and modeling of high-pressure phase behavior of binary CO_2-amides systems. *Fluid Phase Equilib.* **2003**, *208*, 53−68.
(91) Liu, K.; Zheng, L.; Wang, Y.; Hou, L.; Ma, Y. Phase equilibrium model and partial molar volume calculations for dimethylformamide and CO_2 binary mixture at high pressure. *Proc. Int. Conf. Mater. Renewable Energy Environ.* **2011**, *2*, 1478−1482.
(92) Zúñiga-Moreno, A.; Galicia-Luna, L. A. Compressed liquid density and excess volumes for the binary system CO_2 + **N,N**-Dimethylformamide (DMF) from (313 to 363) K and pressures up to 25 MPa. *J. Chem. Eng. Data* **2005**, *50*, 1224−1233.